TRACING DUST PROVENANCE, CYCLING, AND HISTORY IN THE WASATCH MOUNTAINS USING STRONTIUM ISOTOPES AND TREE RINGS

by

Olivia Leigh Miller

A thesis submitted to the faculty of
The University of Utah
in partial fulfillment of the requirements for the degree of

Master of Science

in

Geology

Department of Geology and Geophysics

University of Utah

August 2013

The University of Utah Graduate School

STATEMENT OF THESIS APPROVAL

The thesis of **Olivia Leigh Miller**

has been approved by the following supervisory committee members:

D. Kip Solomon	, Chair	**5/31/13** Date Approved
Thure E. Cerling	, Member	**6/3/12** Date Approved
David R. Bowling	, Member	**5/29/13** Date Approved

and by **D. Kip Solomon** , Chair of

the Department of **Geology and Geophysics**

and by Donna M. White, Interim Dean of The Graduate School.

ABSTRACT

To further our understanding of dust cycling from the Great Basin to the Rocky Mountains, this study uses strontium concentrations and isotopes ($^{87}Sr/^{86}Sr$) to investigate provenance of dust landing on the Wasatch Mountains and to determine that a dust strontium record is preserved in tree rings. To do this, the strontium isotopic signature of dust landing on the Wasatch Mountains, tree rings, soil, and bedrock have been measured. The tree ring isotopic signature is a reflection of how strontium from dust and bedrock mix within the soil. This can then be used to trace changes in dust sources through time via tree rings. A large fraction of the strontium in soil and tree rings comes from dust, although some bedrock dependent variation exists. Trees get a majority of their strontium from dust, making them a useful record of dust source and deposition. Over time, a tree growing over the Tintic Quartzite shows changes in strontium source, which are interpreted as changes in dust source.

TABLE OF CONTENTS

LIST OF FIGURES

LIST OF TABLES

ACKNOWLEDGEMENTS

I wish to thank my thesis committee members, D. Kip Solomon, Thure Cerling, and David Bowling, for their thoughtful suggestions and guidance. I am very grateful to Diego Fernandez for his extensive support of my method development and laboratory analysis, as well as Chris Anderson and Shawn Thomas for help in the lab. Thanks also to David Coyne and Fletcher Reed for their assistance in sample collection. I would like to acknowledge Scott Hynek and Glen Mackey for their intellectual input and Blake Wellard and Mitch Powers for their insight into dendrochronology. Thank you to the Global Change and Sustainability Center for support through the GCSC Fellowship, IsoCamp, and the effort to foster an interdisciplinary community.

INTRODUCTION

This study uses strontium concentrations and isotopes ($^{87}Sr/^{86}Sr$) to investigate provenance of dust landing on the Wasatch Mountains and to determine if a dust strontium record is preserved in tree rings. To do this, the strontium isotopic signature of dust landing on the Wasatch Mountains, bedrock, and tree rings has been measured. The tree ring isotopic signature will be a reflection of how strontium from dust and bedrock mix within the soil. This can then be used to trace changes in dust sources through time via tree rings. As the population in the Great Basin grows, so do disturbances of fragile desert soils and demands on groundwater resources that could lead to soils drying and increased dust production. This study contributes to our understanding of dust transport patterns from the Great Basin to the Rocky Mountains before major water development of groundwater resources and of the impact of groundwater use on rural and major urban areas.

Strontium isotopic ratios of dust depend on the geology of the region of origin, rendering strontium a powerful tracer for atmospheric material such as dust. This study uses strontium isotope signatures as both a dust provenance and, more loosely, historic environmental indicator, as changes in dust sources reflect changes in climate and land use. Strontium has been used to trace dust sources and transport patterns (Graustein and Armstrong, 1983; Grousset and Biscaye, 2005). Dust transport tracks can be mapped using satellite imagery, weather measurements, and air-mass back trajectories. The

isotopic signature of dust, matched with meteorological data, can indicate the unique provenance signature of dust landing in the Wasatch Mountains. This characterization of dust provenance can then be compared to the strontium isotopic ratios found in tree rings to understand changes in dust sources through time. Strontium isotopes have also been used to trace nutrient sources in vegetation (Gosz et al., 1983; Graustein and Armstrong, 1983; Reynolds et al., 2012).

Tree rings can be used as archives of past environments. Tree rings can be used as temporal monitors of environmental change because they create annual growth rings. In the spring rapid growth produces a light-colored earlywood, and in the summer and fall slower growth produces darker late wood (Watmough, 1999). Annual ring formation allows for very accurate dating, making trees sensitive biomonitors of environmental changes. Scientists have used tree ring widths, density, patterns, and scars to understand past precipitation, temperature, fire regimes, floods, earthquakes, avalanches, glaciations, and solar patterns (Amato, 1988).

Understanding dust deposition in the Wasatch Mountains is important as it indicates atmospheric circulation and transport as well as land use and climate in the dust source location. Results from this study are applicable to air quality and human health, quantifying desertification and making predictions about its consequences, understanding effects of land use and related groundwater depletion, exploring strontium in biological cycling, expanding the use of dendrochronology and dendroclimatology, confirming agriculture and livestock implications for dust transport and deposition, appreciating the effects of dust on snowmelt, and expanding the geologic and climate history of the Wasatch Mountains and surrounding areas.

Wind erosion and dust emissions are important components of many ecological processes on local and global scales (Field et al., 2009a). Dust transport redistributes nutrients and organic material to deposition sites (Field et al., 2009b). Soil nutrients such as nitrogen and phosphorous are often associated with smaller soil particles (those that can be transported over long distance through the air). Their movement removes nutrients from source area and enriches nutrients in deposition areas (Li et al., 2007). Many soils in the American Southwest are covered in biological soil crusts that reduce the wind's ability to erode soils (Belnap and Gillette, 1997; Eldridge and Leys, 2003). Disturbed desert soils are less able to protect soils from wind erosion, which removes nutrients from the soil and enhances dust deposition elsewhere (Belnap and Gillette, 1997; Neff et al., 2008). In Utah, dust deposition rates have dramatically increased since the mid-19th century, likely due to increased grazing agriculture, and other human activities (Neff et al., 2008; Reynolds et al., 2010).

The Wasatch Front metropolitan area, home to two million people and growing, relies heavily on snowmelt from the Wasatch Mountains for its water supply. The Salt Lake valley receives approximately 35 cm of precipitation annually, while the neighboring Wasatch Mountains receive over 130 cm of precipitation (Hutchins-Cabibi et al., 2006). Dust can land on, and affect, precious winter snowpacks where mountain snow cover is a vital source of water in an arid region such as Utah. Snowmelt contributes to surface and groundwater, and changes to the snowpack can affect these reservoirs. Salt Lake City also has to contend with severe air quality issues every year, and particulate matter is a strong component of the problem.

Building on this previous work, I have established the basics of the dust strontium

cycle as dust travels from its source to the Wasatch Mountains and becomes incorporated in soil and vegetation. I have established that trees do record the strontium isotopic signal of dust, and that this can be used to trace dust deposition back in time.

In this study, I show that the strontium in dust deposited on the Wasatch Mountains closely resembles the strontium in soils at predicted dust source locations. Then I discuss the strontium in soils formed over different bedrocks to show that soils, which are a mixture of weathered bedrock and atmospheric deposition, are very similar to dust, with respect to strontium. I extend this analysis to trees growing on different bedrocks, to show that trees get most of their strontium from dust, which proves that a strontium dust record is preserved in trees. I describe possible ways to tease out the historical record of dust using tree rings. Some additional elemental data from tree rings are also described.

LITERATURE REVIEW

Strontium as an environmental tracer

The ratio of ^{87}Sr to ^{86} Sr has been used as a tracer of natural processes in the lithosphere and hydrosphere and has proven useful in quantifying atmospheric inputs for an ecosystem (Faure, 1977; Gosz et al., 1983). Strontium has four naturally occurring stable isotopes: ^{84}Sr, ^{86}Sr, ^{87}Sr, and ^{88}Sr. Radiogenic ^{87}Sr is produced through the beta decay of ^{87}Rb ($t_{1/2}$ = 48.8 Ga) (English et al., 2001; Graustein and Armstrong, 1983). Strontium (ionic radius of 1.18 Å) is close to the same size as calcium (1.00 Å), and both are diatomic, so strontium can substitute for calcium within the crystal lattice of all common rock forming minerals (Capo et al., 1998). Rubidium is an alkali metal that occurs in highest abundance in potassium rich minerals such as muscovite, biotite, alkali feldspars, clays, and evaporates. Rubidium has two naturally occurring isotopes, ^{85}Rb and ^{87}Rb. Rubidium (1.52 Å) is close enough in size to substitute for potassium (1.38 Å) within a mineral lattice (Capo et al., 1998). Both potassium and calcium are common elements in many rock-forming minerals, making rubidium and strontium relatively common as well. The isotopic ratio ($^{87}Sr/^{86}Sr$) of a rock varies depending on the age and rock type (with a particular initial $^{87}Rb/^{86}Sr$ ratio) of a region.

The ratio of rubidium to strontium varies due to different chemical and physical properties of the two elements. During fractional crystallization of a magma, strontium tends to solidify earlier, leaving rubidium to become increasingly concentrated in the

residual fluid (Gosz et al., 1983). Rocks with high rubidium concentrations will eventually contain more ^{87}Sr than rocks enriched in strontium. Granite, particularly old granite, will typically have higher $^{87}Sr/^{86}Sr$ ratios while limestone, or a younger rock, will have lower $^{87}Sr/^{86}Sr$ ratios (Gosz et al., 1983).

The $^{87}Sr/^{86}Sr$ ratio of soils and most near surface continental rocks typically lies between 0.709, the ratio in modern ocean water, and about 0.720, the ratio in streams draining ancient Rb-enriched regions, such as the Canadian Shield (Graustein and Armstrong, 1983). In old rocks that are enriched in Rb, such as Precambrian granite, the $^{87}Sr/^{86}Sr$ ratio may be much higher than the crustal average and young volcanic rocks may be depleted in ^{87}Sr (Graustein and Armstrong, 1983). Sedimentary rocks tend towards intermediate ratios (English et al., 2001). Marine limestone $^{87}Sr/^{86}Sr$ ratios vary with time from about 0.7068 to 0.7091, reflecting changes in the strontium isotopic ratio of the ocean (Burke et al., 1982). Strontium ratios of rocks differ in their $^{87}Sr/^{86}Sr$ ratio, depending on rock age and the initial $^{87}Rb/^{86}Sr$ ratio, and these differences are reflected in the $^{87}Sr/^{86}Sr$ ratios of sediments or stream water derived from them (Gosz et al., 1983; Graustein and Armstrong, 1983).

The ratio of $^{87}Sr/^{86}Sr$ is useful as a tracer because it is unique for atmospheric material and can be followed through the ecosystem (Gosz et al., 1983). The ratio of $^{87}Sr/^{86}Sr$ is useful in discriminating different dust source areas (Biscaye et al., 1997). Strontium does not fractionate measurably during biological processes (Gosz et al., 1983). This makes strontium ratios good indicators of the original source of strontium. The $^{88}Sr/^{86}Sr$ ratio is constant and so an analysis of this ratio can be used as a standard to correct for fractionation during measurement (Gosz et al., 1983).

Broadly, strontium in soils comes from weathering of parent material or atmospheric deposition. Deposited dust can contribute strontium to the soil in two ways, the carbonate and labile (soil-water exchangeable fraction) of dust may be dissolved, and the silicate phases in dust may be weathered. Bulk soil, soil waters, and secondary soil minerals maintain the isotopic composition of the parent material, although they can be modified by differential weathering of primary minerals and external sources such as dryfall and precipitation (Capo et al., 1998). Certainly, additional sources and processes can be present, such as climate, biological factors and recycling of organic matter, but as a first approximation, soil formation is a two-component mixing process.

An understanding of the dust, bedrock, or soil component of interest is essential. Some debate exists over which exact fraction of strontium in the soil or rock is most useful to vegetation, and this becomes significant in selecting a leaching method to use prior to isotope analysis. Strontium in dust or soil can be found in numerous locations and multiple definitions exist. They can be defined by the solution used to extract them: the exchangeable fraction, the carbonate fraction, the Fe-Mn oxides fraction, the organic matter fraction, and the residual fraction. These categories can also be defined operationally as the water soluble fraction, the exchangeable fraction, the acid soluble fraction, the amorphous oxides fraction, the manganese oxide bound fraction, the organically bound fraction, the crystalline oxide fraction, and the residual fraction.

Different strengths of extractants target each of these categories. The labile or exchangeable strontium in dust, bedrock, or soil is generally the component of interest for a biogeochemical cycling study and so extractant selection is important in the method development process. Different strengths of acids target different minerals, which can

produce different strontium concentrations and isotopic values, making comparison between different studies potentially difficult. Generally, most studies target the exchangeable, labile, strontium, although some complete an extensive sequential leach starting with a weak leach such as water, and progressively using stronger leaches, to understand the strontium isotope signature of different stages of the weathering process.

Previously, a higher concentration of strontium was required to be able to get measurable $^{87}Sr/^{86}Sr$ ratios and so stronger extractants were typically used. This leads to measurement of not only the exchangeable strontium, but also the easily reducible, organic bound, and the residual fraction strontium to be measured. As mass spectrometry technology has improved and a lower limit of detection can be achieved with smaller samples, the leaching processes of many studies has evolved, and researchers can target just the exchangeable fraction better. They can now use an extractant on a smaller sample size that leaches only the targeted fraction that is the most significant fraction in biogeochemical cycling.

Effects of dust on snowpack duration and trace and major elements

Deposition of dust to the snowpack can affect both the chemistry and albedo of the snow. Snow has the greatest albedo of any natural surface. Dust and other material reduces this albedo, particularly in visible wavelengths (Warren and Wiscombe, 1980). Dust in snow increases absorbed solar radiation and melt rates (Conway et al., 1996). Recent research indicates that dust increases radiative forcing and decreases snow cover duration. In the San Juan Mountains, dust was found to shorten snow duration by 18-35 days during the ablation period (Painter et al., 2007). The duration of snow in mountain

regions is an important control on the timing and magnitude of water supplies, power generation, agriculture timing, and forest fire regimes (Westerling et al., 2006) and so changes to runoff timing can have significant effects on these resources.

Dust has also been shown to significantly affect snowpack chemistry (Bacardit and Camarero, 2010). In the Fraser Experimental Forest, a dust event increased snow pH, calcium, electrical conductivity, and acid neutralizing capacity (ANC) (Rhoades et al., 2010). Atmospheric dust commonly contains calcite, which dissolves and neutralizes acidic inputs to the snow (Rhoades et al., 2010). Dust inputs doubled the P (phosphorus) content of surface soils and enriched levels of carbonate, Ca (calcium), Mg (magnesium), K (potassium), Na (sodium), and various micronutrients of Colorado Plateau ecosystems (Reynolds et al., 2001; Reynolds et al., 2006). More locally, in the Wasatch Mountains, trace elements, major anions, ANC, and pH increase in snow post dust deposition (Carling et al., 2012).

Dust in the Wasatch Mountains

The Wasatch Mountains were the easternmost boundary for Lake Bonneville. Lake deposits from Lake Bonneville now serve as a significant source of dust that, under certain conditions, can be uplifted, transported, and deposited on the Wasatch Mountains. Dust emission sources for the Wasatch Mountains are located mostly in low-elevation late Pleistocene to Holocene alluvial environments in southern and western Utah and southern and western Nevada (Steenburgh et al., 2012).

Visible dust events in the central Wasatch Mountains are associated with synoptic cold fronts, baroclinic troughs, and airmass convection (Steenburgh et al., 2012). Dust

event occurrence peaks in the Spring (April) with another smaller peak in the fall (September) (Steenburgh et al., 2012). The average annual dust flux is 400 g/m^2, with a maximum annual dust flux in 1935 of 2800 g/m^2 (Steenburgh et al., 2012). For March-May, mean monthly total dust flux is 237 g/m^2, representing about 59% of the mean annual total dust flux (Steenburgh et al., 2012). While this study has a bias towards visible dust events, the dust from such events is the dust of concern for snowpack duration. Due to the significant dust deposition the Wasatch Mountains receives, dust will likely be a significant source of strontium and calcium in the montane ecosystem.

Understanding dust systems in the Wasatch has important implications for air quality and human health. The Environmental Protection Agency has designated two sizes of particulate matter to be monitored as part of the National Ambient Air Quality Standards, as required by the Clean Air Act. The particulate matter sizes are PM10 (less than 10 um diameter) and PM2.5 (less than 2.5 um diameter) (UDAQ, 2011). PM10 is typically associated with wind-blown dust while PM2.5 is typically associated with combustion reactions. Sources include burning of gasoline, natural gas, coal, oil, and other fuels, industrial plants, agriculture (plowing or burning fields), unpaved roads, mining, construction, and reactions of VOCs, NO_x, SO_x, and other air pollutants. Particulate matter in the air can cause nose and throat irritation, lung damage, bronchitis, and early death. It is also the main source of haze that reduces visibility (UDAQ, 2011).

Dendrochemistry

Dendrochemistry is the study of elemental and chemical distribution in tree rings to make spatial and historical estimates of element availabilities and to understand the

physiological processes that control the uptake, transport, and sequestration of elements in secondary xylem (Speer, 2010). Trees take up nutrients through their bark, leaves, and roots (Speer, 2010). Trees take up heavy metals that can travel with ligands, soluble organic compounds, and become fixed as part of cell walls (Speer, 2010). Basic assumptions of dendrochemistry are that mineral distribution is stable and that the chemical composition of the annual growth ring at least partly reflects the chemistry of the environment during the year of formation. For example, Watmough and Hutchinson (1996) have confirmed the relationship between trace metal deposition and changes in metal concentrations in tree rings at a given site. Related studies have used isotopes or trace metals in tree rings as markers of atmospheric and soil heavy and trace metal pollution (Sheppard and Funk, 1975; Watmough, 1999; Watmough and Hutchinson, 1996), soil acidity (Chen et al., 2010), and nuclear fallout (Kagawa et al., 2002; Katayama et al., 2006).

Some studies using dendroanalysis have succeeded while others have failed due to tree physiology and metal mobility (Donnelly et al., 1990). Barnes (1976) found very little correlation between tree ring age and air borne lead concentrations. While investigating the potential of red spruce trees for use in tracing heavy metal atmospheric pollution, Zayed (1992) found large variations in metal concentrations in tree rings and concluded that red spruce is not a sensitive bio-indicator of atmospheric metal pollution. Lukaszewski (1988) found no increase in metal concentrations within tree rings despite the beginning of industrialization. Hagemeyer (2000) identified changes in radial distribution of elements over time as well as remobilization and translocation of elements in tree rings and concluded that element distribution in tree rings should not be used for

biomonitoring. Legge et al. (1984) argue that conifers record environmental signals better due to the primitive nature of the wood. They note that conifers poses tracheids and only a few ray cells, as opposed to hardwoods, which possess vessels and many medium to long ray cells. These cells are involved in elemental translocation, and fewer ray cells should reduce translocation. Of note is that all of these studies looked at elemental concentrations alone, and did not investigate isotopic changes.

Strontium biogeochemical cycling

Strontium in a forest is derived from two sources, weathering, and inputs from the atmosphere, although the dominant source is unknown. Eghbal (1993); Rabenhorst (1984), and West (1988) argue that parent rock is the most significant source of carbonates (and thus calcium and strontium) in soil. Other researchers argue that dust is the most significant source (and thus strontium) (Capo and Chadwick, 1999; Chiquet et al., 1999; Dart et al., 2004; Stewart et al., 1998; Van der Hoven and Quade, 2002). The rate of bedrock weathering can influence the amount of atmospheric influence on a tree. Trees growing over rapidly weathering bedrock will see more of a chemical influence from the bedrock than trees growing over slowly weathering bedrock, such as the arid Southwestern US (Cutter and Guyette, 1993). Trees growing in shallow soils will also be more sensitive to atmospheric inputs due to the high ratio of land surface to volume (Cutter and Guyette, 1993).

Some researchers estimate that up to 80-90% of the strontium in the organic matter of the soil comes from the atmosphere (Graustein and Armstrong, 1983), (Gosz et al., 1983). English et al. (2001) measured $^{87}Sr/^{86}Sr$ in trees growing on different

substrates (Precambrian granite, Paleozoic limestone and sandstone, Tertiary sandstone and basalt, and Pliocene basalt, and andesite) and found very little difference in the tree $^{87}Sr/^{86}Sr$ ratios within one mountain range but much greater differences between mountain ranges, which they attribute to the overriding influence of local and regional atmospheric dust sources of strontium. The $^{87}Sr/^{86}Sr$ deposited in woody tissue should be representative of the $^{87}Sr/^{86}Sr$ ratios in the available cation pool in the soil at a given time, and as this pool changes, so would the respective tree ring $^{87}Sr/^{86}Sr$ ratio (Gosz et al., 1983). Previous tree ring studies have found up 15 ppm and between 3-6 ppm Sr in tree wood (åberg, 1995; Padilla and Anderson, 2002).

Deposited dust can contribute strontium to the soil in two ways: 1) the carbonate and labile (soil-water exchangeable fraction) of dust may be dissolved, and 2) the silicate phases in dust may be weathered (Naiman et al., 2000). This first mechanism is likely more significant in the Wasatch Mountains as carbonate dust fluxes are high and carbonates weather at greater rates than silicates. Bulk soil, soil waters, and secondary soil minerals maintain the isotopic composition of the parent material, although they can be modified by differential weathering of primary minerals and external sources such as dryfall and precipitation (Capo et al., 1998). Calcium, and thus strontium, occurs in soils in mineral form or as ions on the exchange complex or in soil solution (Camberato and Pan, 1999). Within the soil, the most bioavailable and mobile substances are those that are water soluble, exchangeable, or weak acid soluble (Baruah et al., 2011). Previous work has shown that calcium in soils derived from parent material decrease as follows: calcareous sedimentary rock, basic igneous rock, acid igneous rock (Jenny, 1994).

Calcium is an essential macronutrient for plants, and so strontium is present in

vegetation as well. Calcium is an essential plant nutrient, and also serves to neutralize and precipitate acids in sap (Parker and Truog, 1920). Vegetation takes up strontium from both the soil solution (water and ions held within soil by capillary action) and the soil exchange complex (the reservoir of ions attracted to negatively charged surfaces of organic matter and soil minerals) via the roots (Capo et al., 1998). Transport of strontium ions to tree roots occurs by mass flow and diffusion (Camberato and Pan, 1999). Exchangeable calcium has been found to be the dominant form, followed by water soluble and acetic acid soluble calcium (Baruah et al., 2011). Trees can also absorb elements into the xylem through foliage or bark after direct deposition (Cutter and Guyette, 1993). Most, if not all, of the inorganic components of wood are derived from soil solution (Cutter and Guyette, 1993).

Plants take up different elements differently. For example, dicots, legumes, and crucifers have more calcium in them than grasses (Parker and Truog, 1920). A time lag between dust deposition on soils and uptake by roots likely exists due to element adsorption onto soil particles and rate of element transport within the tree. However, this has not been studied extensively. Such a time lag would not exist for elements deposited directly onto the tree (Watmough, 1999). Element uptake is affected by the sapwood-heartwood concentration equilibrium, the quantity of macronutrients versus metals, ion solubility, soil type, and pH (Cutter and Guyette, 1993; Gerloff et al., 1966; Padilla and Anderson, 2002). Biologic processes do not measurably fractionate strontium so the strontium isotopic ratios of vegetation will reflect the strontium isotopic composition of labile cations in the soil (Capo et al., 1998).

Once trees uptake elements, they may translocate, depending on the environment,

xylem characteristics of specific tree species, and element characteristics (Cutter and Guyette, 1993). Element mobility is a function of ion solubility, sapwood-heartwood equilibrium concentrations, charge/ionic radius ratio, essential nature (how essential the element is to the tree), sap pH, and bonding in the xylem matrix (Cutter and Guyette, 1993). Essential elements, such as phosphorous, can be transported from interior rings to outer rings to meet the metabolic needs of the cambium (Speer, 2010). Within an annual ring, strontium has been found to gradually increase from earlywood (wood formed in the spring) to latewood (wood formed in the summer and fall) (Silkin and Ekimova, 2012) although this is within one annual ring, and so an annual record is preserved.

Additionally, strontium is only moderately mobile between active tree rings (rings created within the previous 1-7 years) (Padilla and Anderson, 2002) and multiyear average values may still be preserved. The time scale of translocation is poorly defined. Some researchers claim that strontium does not translocate (English et al., 2001). However, Speer (2010) found that the time scale for translocation is on the order of 3-20 years, and so the general trend in $^{87}Sr/^{86}Sr$ remains. While the analysis of an individual tree ring may not pinpoint a specific year of environmental change, trees still lend themselves to the study of broad environmental changes.

METHODS

Strontium isotopes were used to study the provenance of dust landing on the Wasatch Mountains, its biogeochemical cycling upon deposition, and whether the dust isotopic signal is recorded in tree rings. This was used to develop a dust chronology. The strontium isotopic signature of the ecosystem was characterized (deposited dust, soil, bedrock, and tree material), and mixing models were applied to understand the relative contribution of dust to the soil and trees. Stewart et al. (1998) recommend characterizing the groundwater. However, the sampling sites are located on ridges and are likely groundwater recharge areas. Groundwater that passes through the study site does not flow from elsewhere.

The dust signal was further analyzed by sampling trees and soils overlying three kinds of bedrock (granodiorite, quartzite, and limestone), which can be estimated to have different isotopic ratios. Little to no strontium was expected in the quartzite, so it served as a test of total dust influence for strontium input. The limestone was estimated to have an $^{87}Sr/^{86}Sr$ ratio close to 0.707, which serves as a significant endmember. The granodiorite was estimated to have an $^{87}Sr/^{86}Sr$ ratio between 0.707 and 0.708 (Vogel et al., 2001). Stewart et al. (1998) emphasize that a clear contrast between the isotopic composition of end members be present in order for strontium isotopes to be usefully applied to a soil system.

Dust from visible layers in the snowpack was collected upon deposition and paired with storm tracks to understand if the isotopic signature of dust events from different locations, and thus different geology and respective $^{87}Sr/^{86}Sr$ ratios, can be identified. Strontium was then measured in the same five tree rings from trees growing on three different kinds of bedrock to understand the strontium source. Strontium in three types of bedrock and the respective overlying soil was measured to understand the contribution of strontium in bedrock and dust to soil, and tree rings. Building on the work of Gosz et al. (1983) who measured strontium isotopes in 300-year-old wood, a dust chronology was constructed by measuring the dust strontium isotopic record in tree rings to understand changes in dust sources and soil development.

Elemental concentrations were measured using inductively coupled plasma quadrupole-mass spectrometry on an Agilent 7500ce instrument, and strontium isotope ratios were measured via multicollector inductively coupled plasma mass spectrometry using a Thermo Scientific Neptune. Strontium isotopic measurements were run using the SrFast method, which uses a particular column that filters other elements, specifically rubidium, out and allows only strontium to pass into the ion source. This reduces matrix effects. The sample passes through the column in a 4M HNO_3 solution and strontium sticks to beads covered in organic molecules while the rest of the sample goes to the waste. When the acid is changed to 0.1% HNO_3 and run in the opposite direction through the column, the strontium is released and is transported into the nebulizer. Processing software associated with the Neptune corrects for blanks, interferences (Kr, Rb) and mass bias (using the fixed ratio of ^{88}Sr to ^{86}Sr). Software also calculates measurement error due to counting statistics.

Site description

The Wasatch Mountains run roughly 800 km north to south through northern Utah, forming the western edge of the Rocky Mountains and the eastern (downwind) edge of the Basin and Range Province. Salt lake City lies to the west at an elevation of *ca*. 1300 m, and the central Wasatch Mountains rise abruptly from the valley floor to a peak elevation of over 3400 m.

Three sites were selected to sample dust deposited on snow (Figure 1). Dust sample sites were located with the following criteria in mind: in clearings away from vegetation, canopy drip and throughfall, minimal impact from recreationists, no avalanche debris or slide paths, and away from roads.

Tree cores, soil, and bedrock samples were taken at the Little Cottonwood Canyon site. Slopes at soil sampling sites are steep, and soils are poorly developed. Bedrock types selected are the Granodiorite of the Alta Stock, the Deseret and Gardison limestone (undivided), and the Tintic Quartzite (Figure 2). The granodiorite of the Alta Stock (Oligocene) is described as "light-gray, biotite-hornblende granodiorite of the Alta stock. K-Ar ages of biotite and hornblende and fission-track ages of sphene and zircon are about 33Ma" (Bryant, 1990). The presence of potassium feldspar in the granodiorite will potentially lead to a distinct strontium isotope ratio. The Deseret and Gardison Limestone (undivided, Upper and Lower Mississippian, ~325-355 Ma), are described as "thick-bedded dolomite and limestone locally containing abundant lenses and pods of dark gray chert" and "medium-to dark-grey, thin-to thick-bedded, fossiliferous limestone," respectively (Bryant, 1990). These calcium-rich rocks were selected because of the ease of strontium substitution for calcium, and limestone's ease of weathering. The

Tintic Quartzite (Middle and Lower Cambrian, ~490-550 Ma) is described as "medium to thick-bedded, fine to coarse-grained, white, pale-yellowish-gray, and pale-reddish-brown quartzite" (Bryant, 1990). Little to no strontium is expected in this bedrock type, so it serves as a test of total dust influence for strontium input.

Dust event and meteorological observation

Dust events over the winter of 2011-2012 were observed and dust source identification was attempted using MODIS images, HYSPLIT modeling, meteorological data, and personal observation notes. MODIS images from the Railroad Valley Subset of AERONET were used to identify dust plume sources (NASA/GSFC/Earth Science Data and Information System). HYSPLIT models (Draxler and Rolph, 2012) were used to confirm MODIS images. Meteorological data were obtained from the National Climate Data Center (Salt Lake City International station, hourly observations). The dust observations from this dataset are subjective and were supplemented with personal observation.

Dust sample collection

Samples were collected from individual dust event layers deposited on snow from three sites. Collecting dust from snow isolates the dust from any contamination from underlying soil and, if snow is deposited on top of dust layers, from other dust events. Samples were collected within two weeks of dust deposition, except for dust at the Mill Creek site, which was selected as a site later in the season (March). This site was discovered to collect dust layers well, and dust from each event was collected up to two

months after deposition. Sampling sites were accessed using skis.

At each site a snow pit was dug to obtain information on snow depth, layering, and dust layer depths. Snow above the dust layer was removed and dusty snow was scraped up in LDPE wide-mouth 500mL or 1000 mL plastic bottles (Figure 3). Field blanks were taken by leaving a bottle open for the time necessary to collect samples. Samples were kept frozen until analysis. Samplers wore new powder-free vinyl gloves and nonfibrous clothing to reduce contamination of samples. All plastic-ware used for snow sampling and analysis was acid-washed.

Dust sample analysis

Snow containing dust was melted, filtered to remove organic matter, centrifuged and allowed to settle overnight before excess water was decanted. Dust was allowed to dry in a laminar flow hood for five days, after which it was digested using the cold leach method (Carling et al., 2012), in preparation for strontium abundance and $^{87}Sr/^{86}Sr$ analysis. The cold leach involved leaching the dust in between 2-10 mL 0.8 M HNO_3 (5%v/v) at 22˚C for 24 hours, attempting to attain a 1:500 dilution. Secondary dilutions were prepared for high volume samples, in an attempt to achieve a 1:500 dilution. 100 uL indium (5ppm) was added as an internal standard. To prepare secondary dilutions, dust was separated from primary supernatant and 5% HNO_3 was added to primary supernatant. The cold leach method was selected to allow for comparison with soil samples taken from potential dust sources that had been previously analyzed using this same leach method (Hynek, in press, 2011). Milli-Q water was added to field blank bottles. No acids were added before analysis.

Concentrations of strontium were measured, after 1:10 dilutions of sample aliquot were prepared, using an external calibration curve. These concentrations were used to determine further dilution steps to prepare samples for isotope ratio analysis. A portion of each sample, based on concentration, was pipetted into autosampler tubes and milli-Q water was added to achieve 2 mL, after which 0.667 mL HNO_3 was added to each sample. NIST 987 $SrCO_3$ isotopic standards were prepared at 200 ppb and 30 ppb, and they were run every three samples to check reproducibility. Blanks prepared with 4M HNO_3 were run before every sample.

Snowmelt sample preparation and analysis

Between 30-125mL of snowmelt was decanted from each sample and preserved with 1M HNO_3 for analysis following the same procedures described above.

Tree ring sample collection

To evaluate the influence of dust on soil formation and tree ring strontium isotope composition, tree cores were taken from 10 trees growing on three different bedrock types that are close to each other and to a dust sample collection site (30 trees total). Two cores were taken from the south side of each tree (ten trees/bedrock type) using a 5.15 mm diameter increment borer. Several trees had to be cored on a more easterly side of the tree due to the presence of branches or site topography. Engelmann Spruce, *Picea engelmannii*, were selected as conifers generally have a longer life span and are considered to be more sensitive to atmospheric effects (due to the fact that they have needles all year round and have higher surface area for atmospheric absorption) than

deciduous trees (Padilla and Anderson, 2002). Engelmann Spruce is also a tree commonly found at the sample site. Rooting depths of Engelmann Spruce growing in shallow soils over impervious rocks can be between 1 and 40 cm. Of trees sampled for this study, many had exposed roots, and roots growing directly on rock and within rock cracks. Cores were transported in plastic straws back to the laboratory for drying and analysis.

Tree ring analysis

Cores were allowed to dry before being sanded and rings counted and matched across cores. To compare tree cores, five consecutive rings were selected to analyze from each core. To compare temporal changes within one core, rings were analyzed in groups of five. Tree rings were cleaned in an ultrasonic bath to remove contamination from sanding and dried prior to microwave digestion using 2.5 mL clean concentrated HNO_3 and 0.625 mL hydrogen peroxide (30%). Secondary dilutions were prepared using 201 uL of primary sample digest, 51.2 uL indium (5ppm) internal standard, and 201.5 uL water (1:8.28 dilution) for cross-core comparison. Secondary dilutions for chronological comparison were prepared in a similar manner, using a 1:10 dilution. An external calibration curve was developed, and one blank before and after the USGS standard reference solution T-205, used as an external standard, were measured between sets of five samples.

To concentrate strontium abundances and to remove concentrated HNO_3 so that samples could be inlet into the mass spectrometer in the required 4M HNO_3, primaries were evaporated on a hot plate. Immediately prior to sample inlet, dried samples were re-

acidified with 2.67 mL 4M HNO_3. NIST 987 $SrCO_3$ isotopic standards, prepared at 66 ppb, were run every three samples to check reproducibility. Blanks were run between every sample and standard.

Bedrock and soil sample collection

In order to test whether dust affects the strontium isotope ratio of tree rings, the strontium in bedrock and soil was measured as well. Float rock samples and soil samples were taken from below each tree on each bedrock type. Soil samples were taken from 10 cm depth, 1 m from the tree, on the south side of the tree. Some variability exists within sample location specifics due to individual site variability, including thin soils, and vegetation and outcrop presence. The strontium in dust, bedrock, and soil was compared to the strontium in tree rings to determine how much the dust was influencing soil composition and tree-ring composition.

Soil analysis

Two soil samples from each bedrock type were sieved to remove large pieces and organic material. After soils were allowed to dry, 20 mL of 1M acetic acid was added to 1g of soil and allowed to leach for 24 hours on a shaker table. Acetic acid was selected to mimic the natural carbonic acids produced by vegetation. Samples were then centrifuged, and 5 mL of primary leachate was removed and evaporated to remove the acetic acid. Dried leachate was acidified with 5 mL clean 5% HNO_3. Secondary dilutions were prepared using 5mL 5% HNO_3, 100 uL 5ppm In, and either 100 uL primary leachate for soils over quartzite and granodiorite or 20 uL primary leachate for soils over limestone. A

blank was prepared and underwent all of the same steps to confirm that the acetic acid was clean. One blank before and after the USGS standard reference solution T-205, used as an external standard, were measured between sets of five samples. Secondary dilutions were then analyzed for strontium isotopes. NIST 987 $SrCO_3$ isotopic standards, prepared at 66 ppb, were run every three samples to check reproducibility. Blanks were run between every sample and standard.

Bedrock analysis

Two quartzite and two granodiorite rock samples were cut to remove the outer weathered rinds and expose only pristine rock. Limestone was not analyzed because the isotopic analysis of strontium in tree rings indicated that trees growing on limestone would be poor candidates to use for a dust chronology due to the large contribution of strontium from bedrock. Additionally, strontium concentrations and $^{87}Sr/^{86}Sr$ can be estimated from previous studies (Capo et al., 1998; Edmond, 1992). Chips of these unweathered samples were powdered with an agate mortar and pestle before undergoing the same leach process described in the soil analysis section.

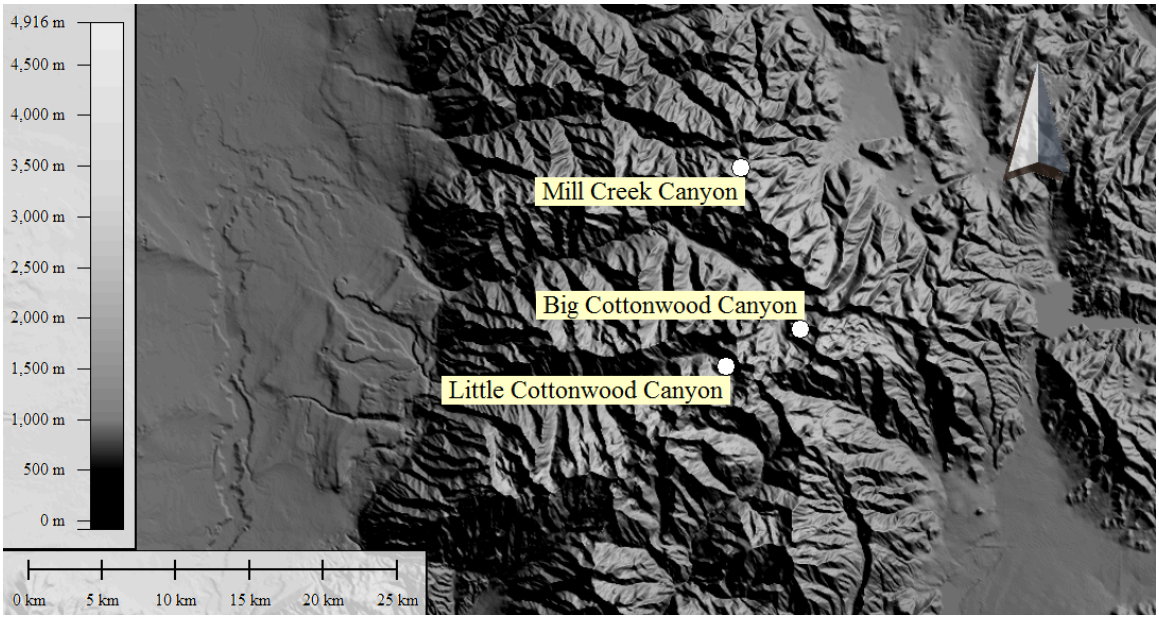

Dust Sample Site	Approximate Elevation (m)	Aspect	Latitude, longitude
Mill Creek Canyon	2913	W	40.670711, -111.603026
Big Cottonwood Canyon (Hidden Canyon)	2840	SW	40.604048, -111.571054
Little Cottonwood Canyon (Grizzly Gulch)	2828	Flat	40.595478, -111.62015

Figure 1. Map and description of sample sites. Dust was collected at all three sites. Tree cores, soil, and bedrock samples were collected at Little Cottonwood Canyon site. The Big Cottonwood Canyon site is referred to as Big Cottonwood Canyon and Hidden Canyon throughout the text.

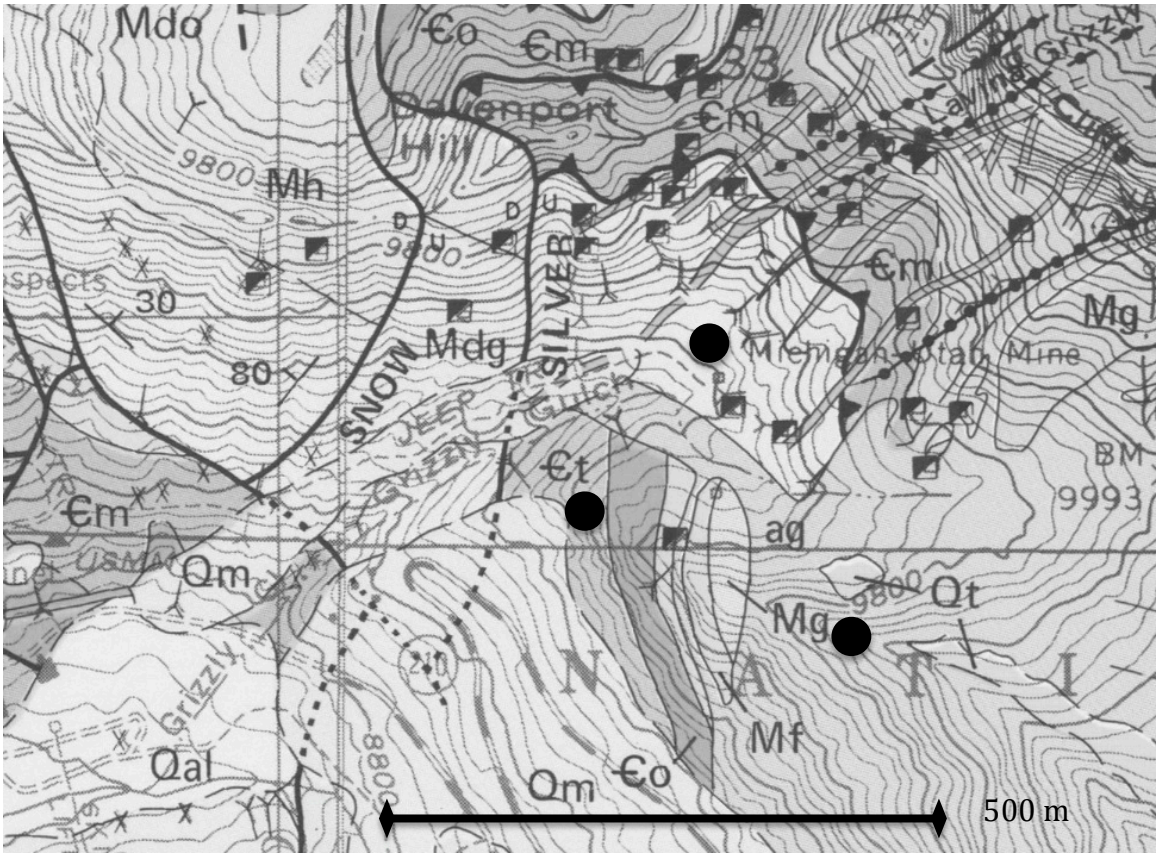

Figure 2. Geologic map of Little Cottonwood Canyon site. Tree core, rock, and soil samples were taken. Rock samples were taken of Alta Stock Granodiorite, Deseret and Gardison Limestone (undifferentiated), and Tintic Quartzite. Soil samples were taken of soils formed over the three bedrock types. Ten trees growing over each bedrock type were cored twice. Map adapted from (James et al., 1978).

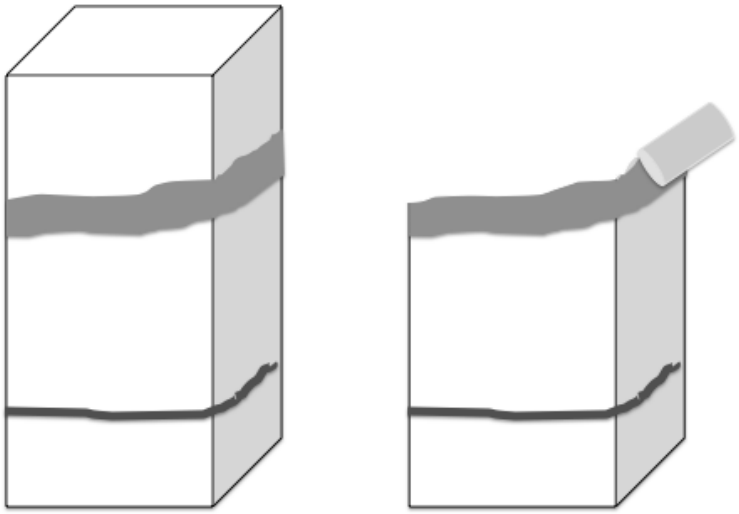

Figure 3. Bottle scrape method. This method was used to collect dust within the snowpack.

RESULTS

Dust event meteorology

For the Wasatch Mountains, the 2011-2012 winter was characterized by very dry conditions, which contributed to drought throughout the summer and fall. The greatest snow depth occurred roughly March 18th, with 254 cm of snow. Snow at the Snowbird SNOTEL site lasted until May 30, 2012. Typically, snowpack lasts several weeks longer than this. Peak snow water equivalent (SWE) is a common measure of the time when snow ablation begins to be greater than snow accumulation. As of April 1, 2012, the typical date of peak snow-water equivalent used in streamflow forecasting, snowpack in the Wasatch Mountains was between 50-69% of average 1971-2000 snowpack (Center, 2012).

Eight dust events, defined as creating a visible dust layer in the snowpack, were observed over the period from December 2011 to March 2012 (Table 1). However, only dust samples from five events were large enough to analyze from all site (D1, D2, D3, D4, and D8). Sample analysis for some events (D5, D6) was possible for some sites. D7 was omitted from further study due to low sample mass at all sites. The snowpack was isothermal at the Mill Creek Canyon site on March 24, 2012. Peak SWE occurred between March 14 and March 29 from SNOTEL data at the Brighton, and Mill D North sites, and between April 13 and 28 at the Snowbird site. The Brighton SNOTEL site is located at 2267 m, the Mill D North site is located at 2733 m, and the Snowbird site is

located at 2938 m. While the Brighton and Mill D SNOTEL sites are located at a closer proximity to the Mill Creek Canyon and Big Cottonwood Canyon sampling sites, the Snowbird site is the closest in elevation to the sample sites and is likely the best reasonable representation of sampling sites.

Due to low snow abundances, dust events after D8 were unusable as dust events fell directly on top of previous dust layers in the snow, and there was no snow in between dust events to isolate layers. This led to the omission of several dust events during the main dust season. However, numerous dust events were deposited earlier in the winter, which were isolated in the snowpack by snow layers, and were thus useable in this study.

Sources of two events were unidentifiable using MODIS images (D1, D4). Observed sources include the Great Salt Lake Desert (GSL Desert), the Salt Flats, the West Desert, the Sevier Desert, and Cason Sink, NV. On days when dust events occur, wind speeds ranged from 3 to 40 mph, with gusts between 21 and 59 mph. Of the times when dust event timing was determinable, dust events tend to begin mid-day to early afternoon. Wind direction ranged from 160 to 10 (south to north).

Strontium results

Dust and snow sampling methods proved to be clean. As shown in the field blanks, sampling methods were clean, and no strontium contamination occurred (Table 2)

Based on strontium concentrations and $^{87}Sr/^{86}Sr$ ratios, samples of individual dust events tend to cluster together within a larger range in dust $^{87}Sr/^{86}Sr$ ratios of 0.71020 to 0.71236 (or 0.71165 when median absolute deviation, MAD, is used to remove outliers) and concentration range of 15 to 1573 ppm (or 111 when MAD is used) (Figure 4). For a

given event, there is little spatial variability in dust deposited across the different sampling sites. Dust samples from the same event but different locations have similar $^{87}Sr/^{86}Sr$ ratios, although the Mill Creek site is the largest outlier for this pattern. There is greater temporal $^{87}Sr/^{86}Sr$ variation than spatial variation, except for a few samples from the Mill Creek site. These dust samples fall within the range of Sevier Desert soil samples that represent potential dust source areas (Hynek, in press, 2011).

The relationship between the $^{87}Sr/^{86}Sr$ ratio in snowmelt and dust is almost a 1:1 relationship, with a slope = 1.0, $r^2 = 0.83$ (Figure 5). This indicates that there is little to no evidence for isotopic fractionation in the melting process, although there is enough scatter in the data that it cannot be completely ruled out. However, strontium fractionation due to phase change is immeasurable (Van der Hoven and Quade, 2002). As the snow melts, the $^{87}Sr/^{86}Sr$ ratio of the snowmelt is the same as that dust. However, the snowmelt strontium concentration, which has been normalized to mass of dust per liter of snow, is much greater. This end product of the dust deposition on snow, incorporation into soil, partial removal by runoff, and dissolution into soil solution, is what the vegetation ultimately has available to draw from. This includes the water-soluble fraction (snowmelt) and acid-soluble fractions (referred to as dust throughout this paper). Total dust refers to combined snowmelt and dust fractions.

Comparing tree samples growing on three different bedrock types reveals notable patterns in the source of strontium for trees (Figure 6). Trees growing on quartzite and granodiorite appear to source their strontium from dust while some trees growing on limestone get their strontium from dust and some trees growing on limestone get their strontium from the weathered bedrock. The trees growing on granodiorite and quartzite

have similar, and higher, $^{87}Sr/^{86}Sr$ ratios than the trees growing on limestone. When compared to the strontium in the underlying bedrock and soil, the pattern for strontium coming from dust becomes even more apparent, as discussed later. The limestone bedrock was not analyzed and so only a general analysis of that system is possible. Because average $^{87}Sr/^{86}Sr$ ratios for marine limestone formed between 325 and 350 Ma range from 0.7075 and 0.7080, and average strontium concentration for carbonates is 610 ppm, general assessments can be made about the limestone system (Capo et al., 1998; Edmond, 1992).

To understand some of the natural heterogeneity of the tree rings, cores from the same tree were compared with each other for both strontium concentration and $^{87}Sr/^{86}Sr$ ratio. The same five rings taken from two cores from the same trees match moderately well for strontium concentration and very well for $^{87}Sr/^{86}Sr$ ratio.

When comparing the strontium concentrations from two cores of the same tree, some variability exists (Figure 7). Two cores from the same tree growing on limestone and quartzite have a nearly 1:1 relationship between the strontium concentrations, while two cores from the same tree growing on granodiorite have a weaker relationship. The geometric mean regression is useful when either variable could be the independent variable because it minimizes the vertical and horizontal residuals, not just the vertical residuals as occurs when using the ordinary least squares regression (Zobitz et al., 2006). For trees growing on limestone, the slope of a geometric mean regression is 0.96 and the r^2 is 0.78. For trees growing on quartzite, the slope of a geometric mean regression is 1.02 and the r^2 is 0.65. For trees growing on granodiorite, the slope of a geometric mean regression is 0.73 and the r^2 value is 0.03. For all trees, regardless of bedrock type, slope

of a geometric mean regression is 1.01, $r^2 = 0.68$. Natural heterogeneity of strontium concentration within the same five rings in two cores from the same tree is variable, depending on bedrock type. Disregarding bedrock type, natural heterogeneity exists, although it is not very strong.

The isotopes show less natural heterogeneity (Figure 8). For trees growing on limestone, the slope of a geometric mean regression is 0.94 and the r^2 is 0.95. For trees growing on quartzite, the slope of a geometric mean regression is 1.05 and the r^2 is 0.92. For trees growing on granodiorite, the slope of a geometric mean regression is 0.97 and the r^2 value is 0.96.There is a very close relationship between the $^{87}Sr/^{86}Sr$ ratios in two cores taken from the same tree for trees, regardless of bedrock type (slope of a geometric mean regression = 1.01, $r^2 = 0.98$). This indicates that the strontium isotopic ratio in tree rings is not appreciably affected by natural heterogeneity, and reflects the strontium source well. The Sr/Ca ratio is also very consistent between two cores taken from the same tree. The slope of the geometric mean regression is 1.0 and the $r^2 = 0.85$.

These results support the hypothesis that strontium isotopic ratios can indicate dust sources. However, they also indicate that estimating dust and bedrock contributions to vegetation using two-component mixing models is a complex process as the concentrations vary more. Additionally, as discussed below, strontium concentrations in other material vary significantly as well.

Little variation occurs when tree cores taken on different sides of a tree are compared (Figure 9). All sides have very close $^{87}Sr/^{86}Sr$ ratios and strontium concentrations. While only one tree was sampled on all sides, the $^{87}Sr/^{86}Sr$ ratios range from 0.71025 to 0.71092. The average is 0.71047, and standard deviation is 0.0002.

Concentrations range from 2 ppm to 3.7 ppm, have an average of 3 ppm, and a standard deviation of 0.6 ppm. The largest range in isotopic ratios is between the core taken on the west side of the tree and a core taken on the south side of the tree (G6 West = 0.71092, G6B South = 0.71025). The largest range in strontium concentration is between the core taken on the east side of the tree and one core taken on the south side (G6 East = 3.7 ppm, G6A South = 2 ppm).

Strontium measurements of tree tissue can be used in some cases to distinguish trees growing on different bedrock types. The bedrock dependent variation can be interpreted as changes in strontium source. However, these are not necessarily only bedrock signals preserved in tree tissue. Certain bedrock types seem to allow trees to source their nutrients from dust more than others, as shown in the bedrock, soil, and tree samples. This occurs when bedrock strontium is very different from strontium in vegetation, but strontium in vegetation is very similar to that of dust and soil.

Analyses of soil and rock samples reveal elemental differences (Figure 10). Soil developed on limestone has the most strontium, followed by soil developed on quartzite, and then soil developed on granodiorite. Analysis of quartzite and granodiorite shows that they have similar strontium contents, with quartzite having slightly more strontium than granodiorite. Note that this is an approximation of the strontium available to vegetation. With respect to strontium concentrations, quartzite and granodiorite rock samples are very similar, as are the soils formed above them. However, with respect to $^{87}Sr/^{86}Sr$ ratios, all soils are similar, but quartzite is much more radiogenic than granodiorite.

In comparison to the strontium found in trees growing over the respective, and

different, bedrock and soils, the strontium in the tree tissue is much more similar to strontium found in dust than the underlying bedrock, particularly for the quartzite system. The trend is also found in the granodiorite system.

Mixing models can be used to understand the role of various ecosystem components in the strontium cycle. Analysis of dust, soil, rocks, and trees suggest that dust is a very important source of strontium in this system (Figure 11). The total dust strontium is composed of the water soluble (snowmelt), acid soluble (dust leach), and insoluble (dust grains). The vegetation only sees the water and acid soluble fractions, which together form the total dust end member of the mixing model. Soil samples, regardless of bedrock type they formed over, very strongly resemble dust, while trees have a wider range of isotopic ratios depending on bedrock type, and lower concentrations. Strontium isotopes in tree rings encompass the range of values measured in dust and soils. The granodiorite rock samples have $^{87}Sr/^{86}Sr$ ratios similar to dust (average granodiorite is 0.70921), while the quartzite rock samples have much greater ratios (average quartzite is 0.72950).

Trees growing over quartzite fall next to the mixing line between quartzite and quartzite soil. The strontium isotopic ratios of the trees are within the mixing line range but the strontium concentration in the trees is lower. The same is true for trees growing over granodiorite and limestone. The similar isotopic ratios show that dust is an important component of the strontium in trees (Figure 12).

Despite the strong dust influence, the trees growing over the different rock types are differentiated by the influence of different bedrock types. Samples falling outside of the range of the total dust standard error of the mean are significantly different from dust,

indicating some bedrock influence. However, even though the samples are not identical to dust, they are more similar to dust than to the bedrock they grow over, meaning that the main source of strontium is dust.

The samples can be examined for each bedrock type. For trees growing, and soils formed, over quartzite, dust has a very strong influence on soil (Figure 13). Trees do not fall along the mixing line between bedrock and dust. Although they have the same isotopic ratio, they also have lower strontium concentrations, as compared to dust. Quartzite bedrock has a much higher $^{87}Sr/^{86}Sr$ ratio and lower strontium concentrations than dust and soil.

For trees growing, and soils formed, over granodiorite, dust also has a very strong influence on soil (Figure 14). Similar to the quartzite system, trees do not fall along the mixing line between bedrock and dust. They have the same isotopic ratio, but lower strontium concentration, as compared to dust. Granodiorite bedrock has a lower $^{87}Sr/^{86}Sr$ ratio and lower strontium concentrations than dust and soil.

For a mixture of two end members, the fraction of strontium from one component is given by:

$$\frac{M_1^{Sr}}{M_1^{Sr} + M_2^{Sr}} = \frac{R_m - R_2}{R_1 - R_2} \qquad (1)$$

where R = $^{87}Sr/^{86}Sr$, M_n^{Sr} = the mass of strontium in component n, (Stewart et al., 1998). From this calculation, 94-100% of the strontium in soils over quartzite is from dust, 62-100% of the strontium in soils over granodiorite is from dust, and 71 to 100% of

strontium in soils over limestone is from dust. The range of percentage is calculated using the average, average plus standard error, and average minus standard error of the $^{87}Sr/^{86}Sr$ ratios of total dust, bedrock, and soil measurements. Extending this to trees, 85-100% of the strontium in trees growing over quartzite is from dust, 54 to 100% of strontium in trees growing over granodiorite is from dust, and 24 to 97% of strontium in trees growing over limestone is from dust. The large range of possibilities for the granodiorite system is due to the high variability of bedrock strontium values. The large range of possibilities for the limestone system is due to the trend that the ranges of $^{87}Sr/^{86}Sr$ ratios for trees growing over limestone and total dust overlap, as well as the greater similarity of tree $^{87}Sr/^{86}Sr$ ratios to bedrock $^{87}Sr/^{86}Sr$ ratios.

For a two-component mixing system, the mass contribution of one end member can be calculated using the following equation:

$$\frac{M_1}{M_1+M_2} = \frac{Sr_2(R_{mix}-R_2)}{Sr_2(R_{mix}-R_2)+Sr_1(R_1-R_{mix})} \quad (2)$$

where R = $^{87}Sr/^{86}Sr$, M_n = the mass of component n, and Sr_n = strontium concentration of component n (Stewart et al., 1998). Using this equation to calculate the contribution of dust to soil composition shows that between 99 and 100% of soil over quartzite is dust. Between 27 and 100% of soil over granodiorite is dust. Between 99 and 100% of soil over limestone is dust. For these calculations, the average, average plus standard error, and average minus standard error, of total dust, soil, tree, and bedrock values were used. The minimum estimated contribution of dust to soil formed over quartzite could in part

be explained by the low concentration of strontium in the bedrock. A larger contribution from bedrock is required to see a small change in the $^{87}Sr/^{86}Sr$ ratio. The large range of possible contributions of dust for the granodiorite soil is due to large range of $^{87}Sr/^{86}Sr$ ratios of the bedrock.

To calculate the $^{87}Sr/^{86}Sr$ ratio of a mixture, the following equation can be used (Faure, 1977):

$$R_m = \frac{Sr_a Sr_b (R_b - R_a)}{Sr_m (Sr_a - Sr_b)} + \frac{Sr_a R_a - Sr_b R_b}{(Sr_a - Sr_b)} \quad (3)$$

where $R_n = {}^{87}Sr/^{86}Sr$ of component n and Sr_n = strontium concentration of component n.

This mixing model works well when considering soils as a mixture of bedrock and dust. For soils formed over quartzite, the model predicts an $^{87}Sr/^{86}Sr$ ratio of 0.71261, while the measured value is 0.71126 (a difference of .001). For soils formed over granodiorite, the model predicts an $^{87}Sr/^{86}Sr$ ratio of 0.71087, while the measured value is 0.71086 (a difference of 0.00001), using average soil, total dust, and rock strontium concentrations and $^{87}Sr/^{86}Sr$ ratios. For soils formed over limestone, using average soil, total dust, and rock strontium concentrations and $^{87}Sr/^{86}Sr$ ratios, the model predicts an $^{87}Sr/^{86}Sr$ ratio of 0.65603, while the measured value is 0.71097 (a difference of 0.05). However, using average soil, acid soluble dust, and rock strontium concentrations and $^{87}Sr/^{86}Sr$ ratios, the model predicts an $^{87}Sr/^{86}Sr$ ratio of 0.71106, which differs by only 0.00009, suggesting that either the limestone or dust strontium concentrations is too large, and possibly that trees are accessing the acid soluble dust fraction more (which has

a lower strontium concentration). This limestone scenario uses an estimated strontium concentration, and so the predicted $^{87}Sr/^{86}Sr$ ratio is merely an estimate as well.

This mixing model does not work as well when considering trees as the mixture of dust and soil, mostly due to the strontium concentration differences between rock and dust compared to trees. For example, the model predicts an $^{87}Sr/^{86}Sr$ ratio of trees growing over quartzite to be 0.71820, while the measured $^{87}Sr/^{86}Sr$ ratio is 0.71173 (a difference of .006). For trees over granodiorite, the model predicts an $^{87}Sr/^{86}Sr$ ratio of 0.71034, while the measured value is 0.71084 (a difference of .0004). For trees over limestone, the model predicts an $^{87}Sr/^{86}Sr$ ratio of -0.26, while the measured value is 0.70971 (a difference of 0.9). However, using average soil, acid soluble dust, and rock strontium concentrations and $^{87}Sr/^{86}Sr$ ratios, the model predicts an $^{87}Sr/^{86}Sr$ ratio of 0.76971, which differs by only 0.05, again suggesting that either the limestone or dust strontium concentrations is too large, and that the trees may be accessing the acid soluble dust fraction more. The significant deficit of the limestone system is likely due to poor estimation of the strontium concentration in the limestone.

Dust chronology in tree core

One core, from a tree growing over quartzite, sectioned into five-ring sections, spanning 75 rings, was analyzed to see how strontium changed over time (Figure 15). While strontium concentration in the tree rings decreases over time, from a peak of approximately 11 ppm to near 5 ppm in more recent times, the strontium isotopic ratio has increased over time, from around 0.71180 to a peak of 0.71217 in modern times. Other elements that also decrease nearly sequentially over time include magnesium,

calcium, manganese, barium, and zinc. Certain large departures from the overall trends of strontium isotopic ratio and concentration exist as well.

Over time, the strontium isotopic signature within the tree rings has changed. In the first half of the trees life, $^{87}Sr/^{86}Sr$ ratios were below 0.71197, while in the second half of the trees life, the ratios went above this value. Strontium concentrations have slightly decreased over time. These trends produce two zones of strontium isotopic signature for this tree. Two explanations exist. Either the dust source has changed or the tree has shifted towards sourcing more strontium from bedrock weathering. This could occur as the tree ages, and its roots grow deeper and produce more acids to weather rocks.

Comparing the strontium isotopic changes over time to the mixing plots shows that while the strontium in the tree rings has changed over time, the dominant source does not appear to have shifted very much in the past approximately 75 years (Figure 16). All of these strontium isotopic ratios are at the high end of the total dust range of strontium isotopic ratios, suggesting that the trees are recording a change in dust strontium isotopic signature and dust source. Further, the $^{87}Sr/^{86}Sr$ ratio of the core back in time are all well within the range of $^{87}Sr/^{86}Sr$ ratios for the same five rings in different trees, suggesting that the variation within the core is more related to resolution of the tree core as a proxy and not a shift in sourcing strontium from dust to bedrock.

If we consider the trees as a mixture of bedrock and dust, Equation 2 can also be solved to calculate the $^{87}Sr/^{86}Sr$ ratios of dust at different times. However, we do not have a way to know the dust strontium concentration at different times. Considering the trees as a mixture of bedrock and dust is not a quality model because the measured values for these components do not match predicted values as well as the two-component mixing

model that has been used with soil samples. Additionally, for predicting $^{87}Sr/^{86}Sr$ ratios, the model is very sensitive to concentration changes, particularly within the range of strontium concentrations measured (Figure 17). As the dust strontium concentration increases, the $^{87}Sr/^{86}Sr$ ratios become less sensitive.

Other elemental results

Elemental measurements of tree tissue can be used in some cases to distinguish trees growing on different bedrock types. However, concentrations of many elements in tree tissue do not vary by bedrock type (Figure 18). Of note, calcium concentration does not vary within tree rings by bedrock type. The bedrock dependent variation can be interpreted as changes in source. However, these are not necessarily bedrock signals preserved in tree tissue. Certain bedrock types may allow trees to source their nutrients from dust more than others, as shown in the bedrock, soil, and tree samples.

However, strontium and barium in tree material do vary by bedrock type, suggesting that strontium is an appropriate element to use for tracing bedrock and dust inputs to soil and their subsequent uptake by vegetation (Figure 19). For strontium, trees growing on quartzite have the highest strontium concentrations, followed by trees growing on granodiorite, then trees growing on limestone. There is some overlap when the uncertainty estimate is included. However, there does appear to be a trend in concentration order depending on tree type. For barium, trees growing on quartzite and granodiorite are within the same range of barium concentration, while trees growing on limestone have much lower concentrations.

Additionally, the Sr/Ca ratio and the Ba/Ca ratio show bedrock dependency

(Figure 20). For each, the trees growing on limestone have lower ratios than trees growing on granodiorite or quartzite. Trees growing on quartzite and granodiorite are also distinguishable using the Sr/Ca ratio. The pattern produced by the ratios of Sr/C and Ba/Ca in the leach are very similar to the patterns of calcium, strontium, and barium in the woody tissue. This is expected, as the calcium in all trees is similar, regardless of bedrock type, while strontium and barium in trees vary by bedrock type.

Comparing elemental concentrations to strontium concentrations reveals some additional patterns in the influence of bedrock on vegetative uptake (Figure 21). Tree tissue concentration of many elements in comparison to strontium, including calcium, cannot be used to distinguish trees growing on different types of bedrock. However, certain elements in comparison to strontium concentration, including calcium, magnesium, rubidium, and zinc, can be used to distinguish trees growing on the three different bedrock types included in this study.

The elemental analysis indicates that trees are getting some elements from different sources, either different bedrock types or dust, depending on the bedrock they are growing above (Ba, Sr). However, there are also some elements that seem to come from the same source, regardless of bedrock type (Ca, Fe, Mg, Zn). For some elements, the source is not only bedrock dependent, but also strontium concentration dependent (Ca, Mg, Rb, Zn, Mn, Ba).

Table 1. Dust events of the 2011-2012 winter. Dust events, meteorological conditions, and identified sources for dust events.

Event	Date	Wind Direction (compass degrees)	Wind Speed (mph)	Gusts (mph)	Time	Source Area
D1	12/31/11	180-350	5 to 38	21-47	Can't determine	Unknown
D2	2/23/12	170-360-10	3 to 34	21-25, gusts earlier in the day 29-49	11:30am - 1:00 pm dust blowing off GSL Desert, not directly towards SLC.	GSL Desert
D3	2/25/12	170-330	17 to 40	28-59	After 1:53 pm	Salt Flats, GSL Desert
D4	3/6/12	170-360	5 to 33	21-38	Can't determine	Unknown
D8	3/31/12	160-190	14 to 34	26-44	12:40 pm	West Desert, Carson Sink, NV, Sevier Desert and surrounding area

Table 2. Field blank strontium concentrations taken during dust sampling. FB = field blank, HC = Hidden Canyon, Big Cottonwood Canyon, MC = Mill Creek Canyon, LCC = Little Cottonwood Canyon. Number refers to dust layer collected while field blank was taken.

Field Blank	Sr (ppm)	Analytical Error (2σ)
FB HC4-5	<0	0.006
FB MC 8	0.000	0.006
FB LCC 4-5	<0	0.024
FB MC 1-7	<0	0.006
FB LCC 8	<0	0.006
FB HC 8	<0	0.006
Limit of Detection	0.005	

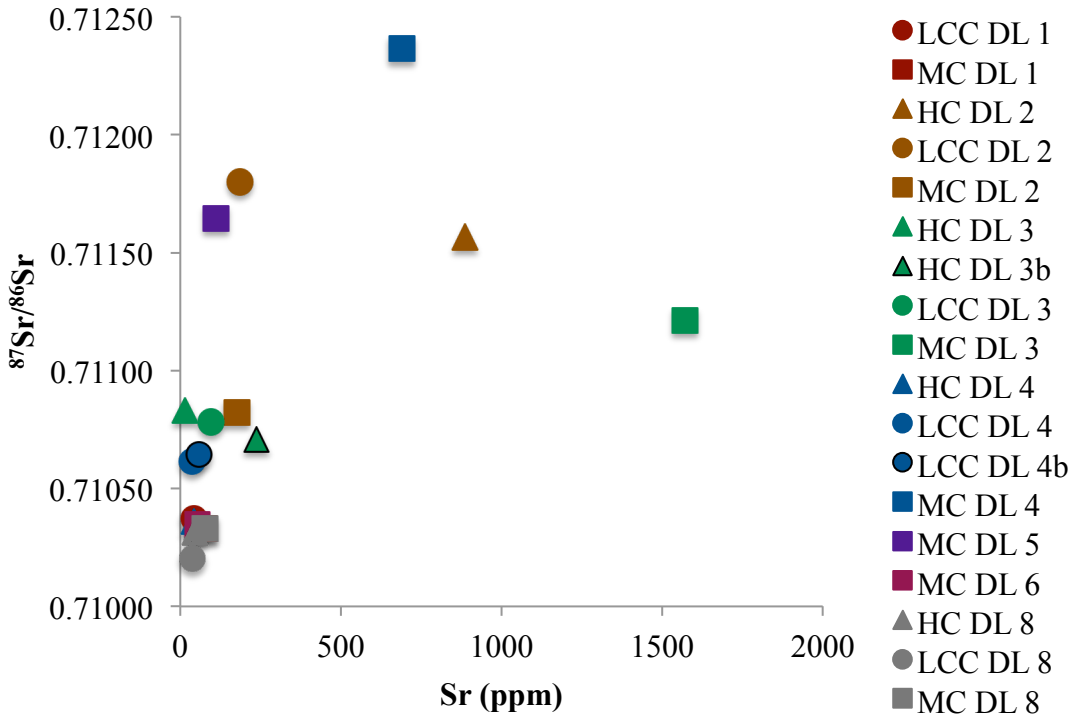

Figure 4. Strontium concentration and $^{87}Sr/^{86}Sr$ ratio of dust events. HC = Hidden Canyon, Big Cottonwood Canyon, MC = Mill Creek Canyon, LCC = Little Cottonwood Canyon. Number refers to dust layer moving up through the snowpack.

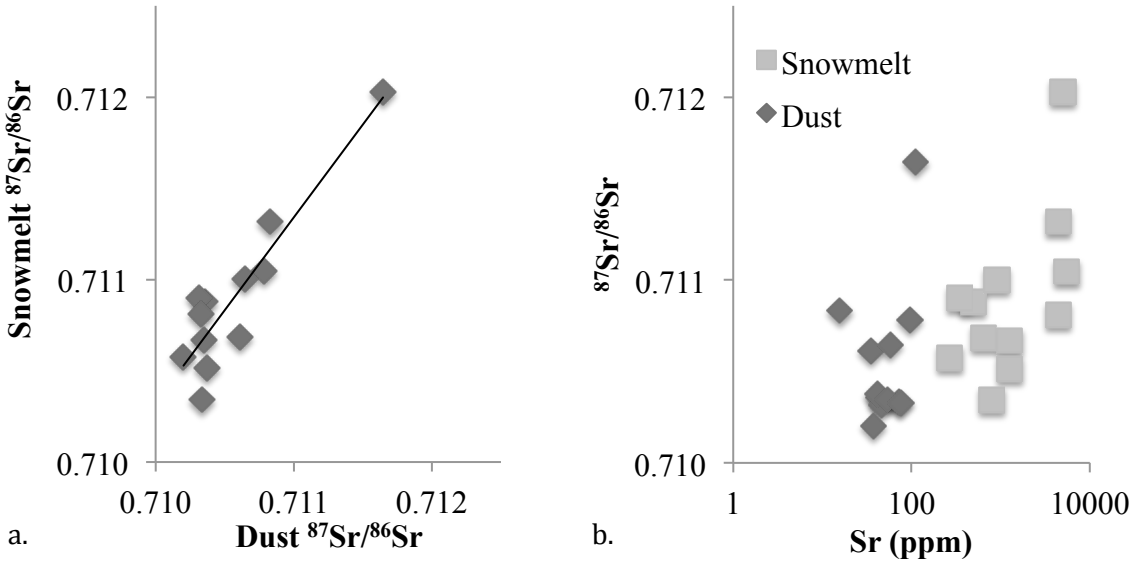

Figure 5. Comparison of acid and water-soluble fractions of dust. The relationship between the isotopic ratio of dust and the snowmelt associated with each dust event is good (slope = 1.0, $r^2 = 0.83$). This indicates that there is little to no measurable isotopic fractionation in the melting process, so the water and dust that goes into soil, and eventually trees, has not undergone isotopic fractionation. However, as shown in b), the strontium in the snowmelt is more concentrated than the strontium in the dust.

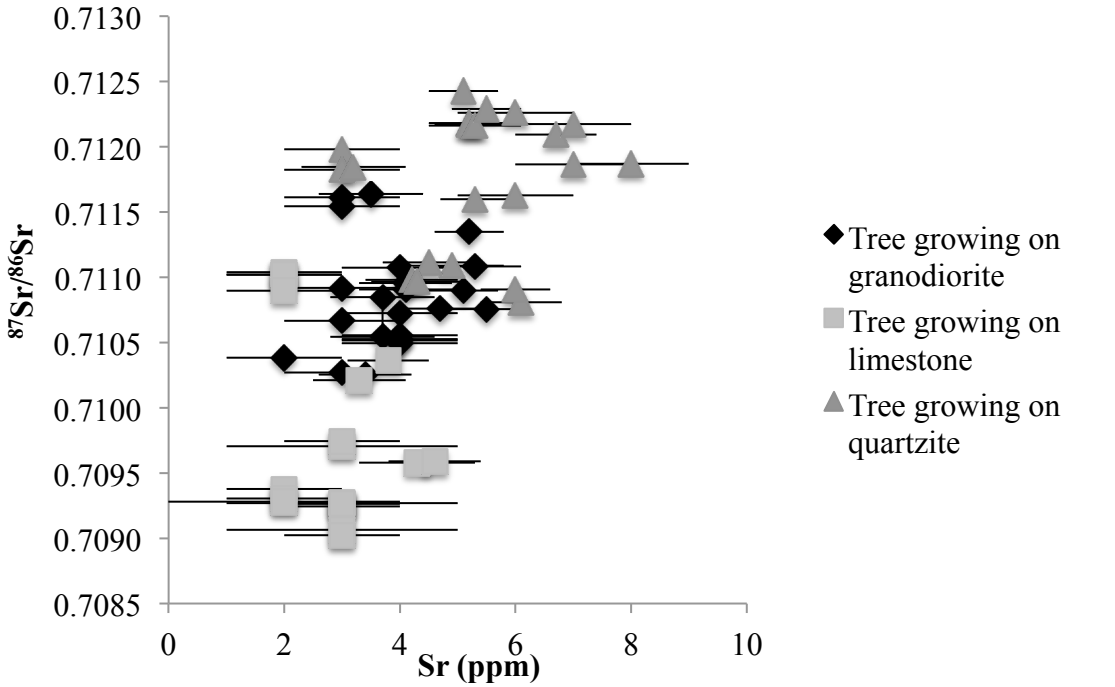

Figure 6. Strontium in trees growing on different bedrocks. Strontium concentration and $^{87}Sr/^{87}Sr$ ratio comparing the same five-ring section from each tree. The strontium varies depending on which rock type the tree grows on.

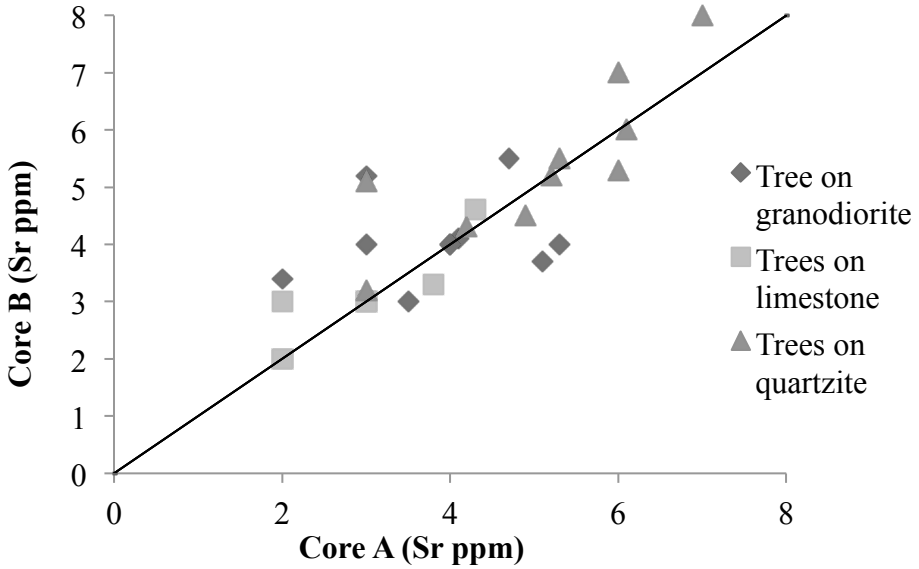

Figure 7. Variation of strontium concentration in woody tissue. Comparison of strontium (ppm) in Core A and Core B of the same tree. Solid line is 1:1 relationship.

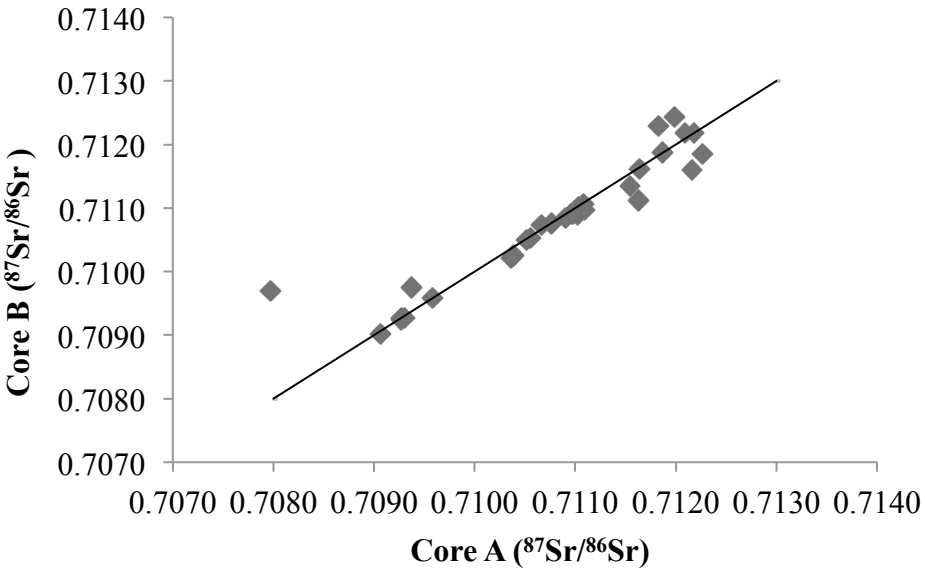

Figure 8. Variation of $^{87}Sr/^{86}Sr$ ratio in woody tissue. $^{87}Sr/^{86}Sr$ ratios in Core A vs. Core B of the same tree. Solid line is 1:1 relationship.

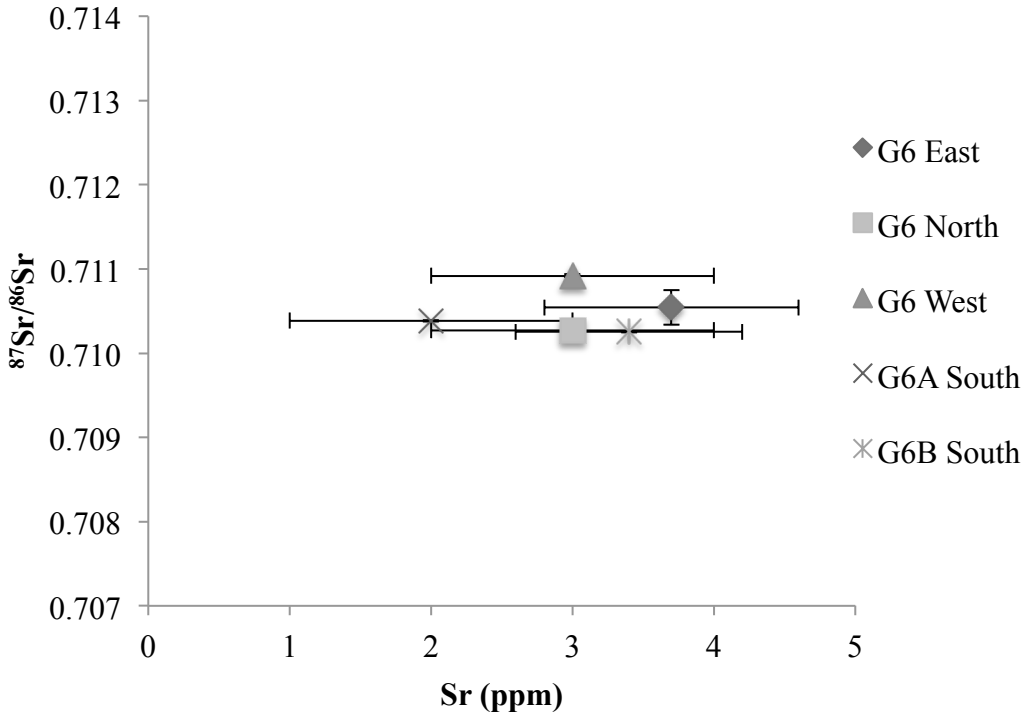

Figure 9. Strontium variation within one tree. Cores were taken from cardinal direction sides of a tree. Two were taken from the south side.

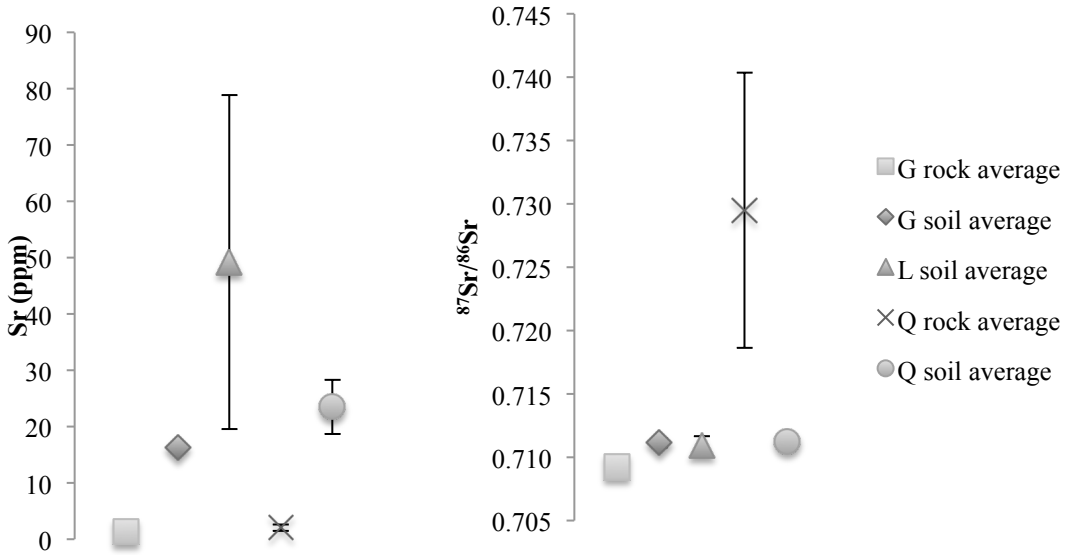

Figure 10. Strontium in soil and bedrock samples. Average strontium concentrations, $^{87}Sr/^{86}Sr$ ratios, and standard deviation for soil and bedrock samples.

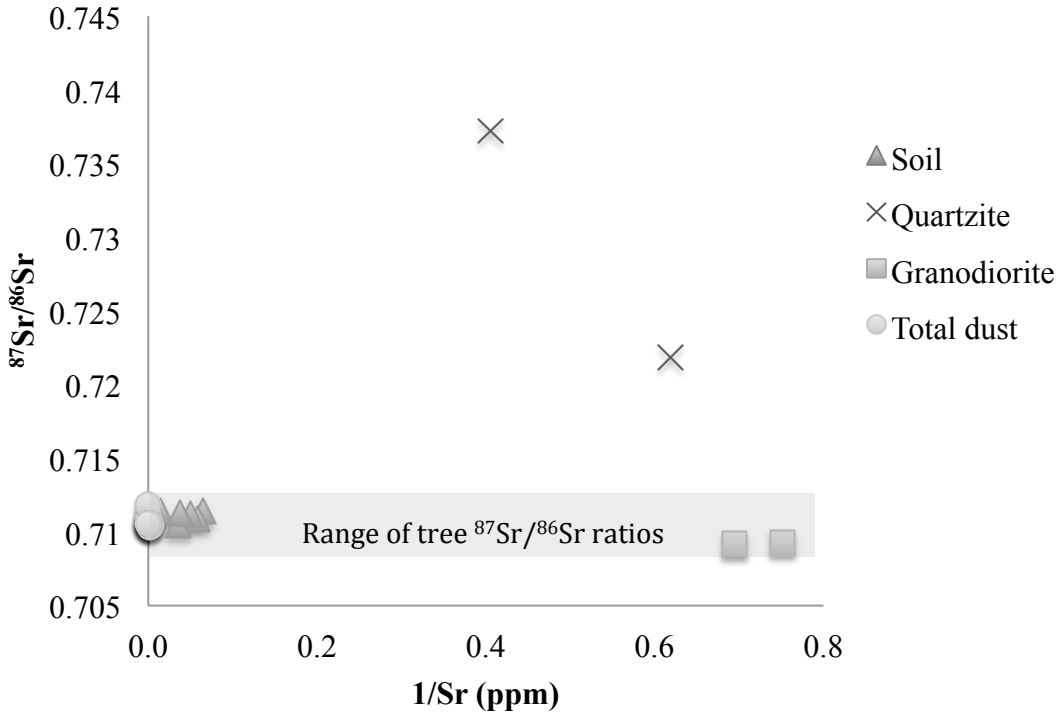

Figure 11. Mixing of all dust, bedrock, and soil samples measured. Tree samples indicate average and range of $^{87}Sr/^{86}Sr$ ratios.

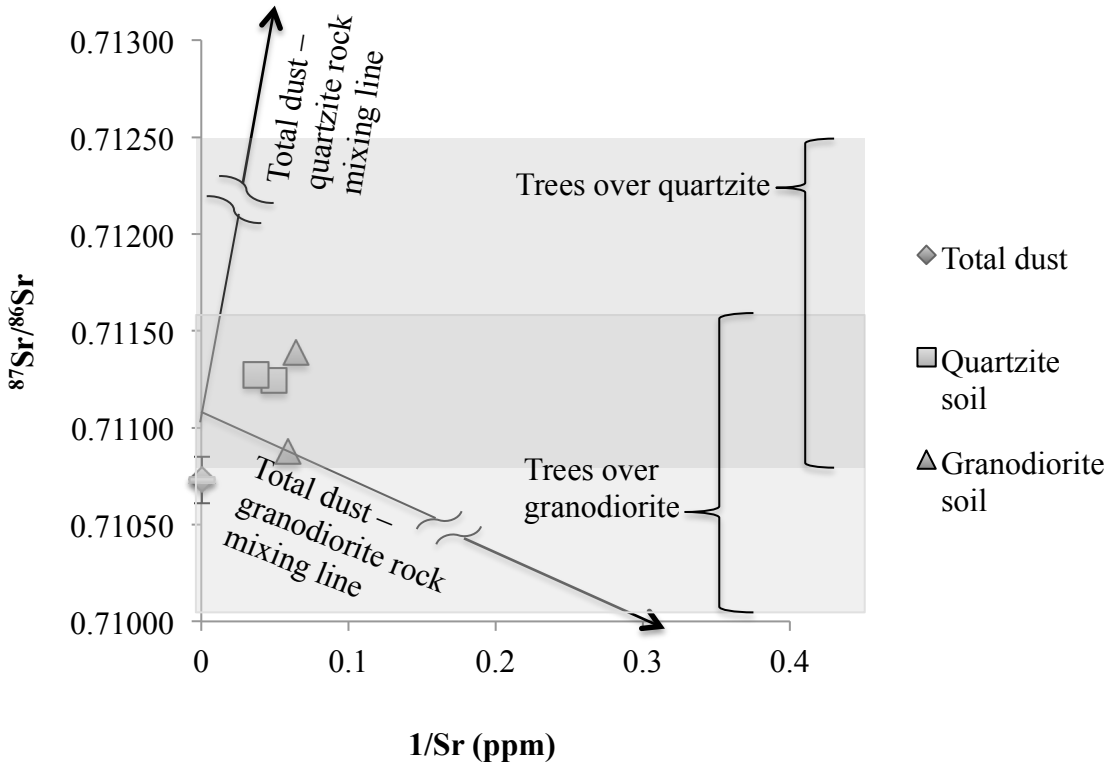

Figure 12. Strontium in quartzite and granodiorite systems. This graph show strontium isotopes and concentrations in dust, soil, and rocks for quartzite and granodiorite systems, as well as strontium isotopes in tree rings. Total dust includes acid and water-soluble strontium. Bars on total dust are the standard error of the mean total dust value, to show difference between other samples. Tree isotope ratios are average and range of all $^{87}Sr/^{86}Sr$ ratios of trees growing over a given rock type. Mixing lines, shown by dark arrows, are between average quartzite rock and soil values, and average granodiorite rock and soil values.

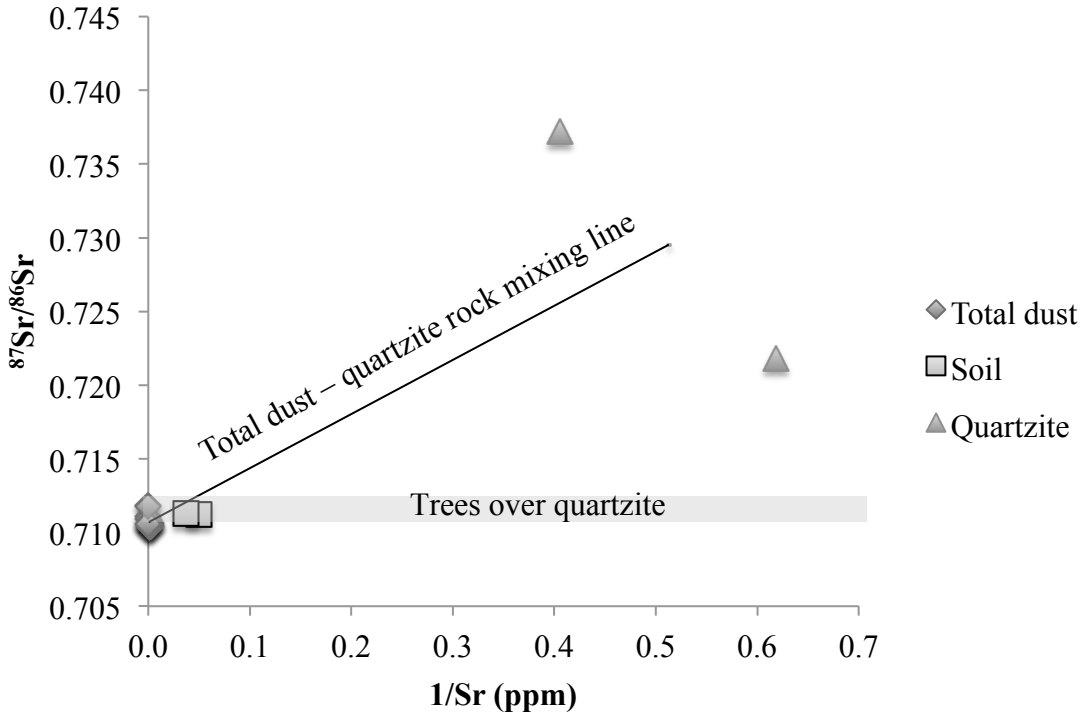

Figure 13. Quartzite system. Mixing of total dust (water and acid soluble fraction) and quartzite bedrock, soil over quartzite, and trees growing over quartzite. Tree data are the average and range of $^{87}Sr/^{86}Sr$ ratio of trees growing over quartzite.

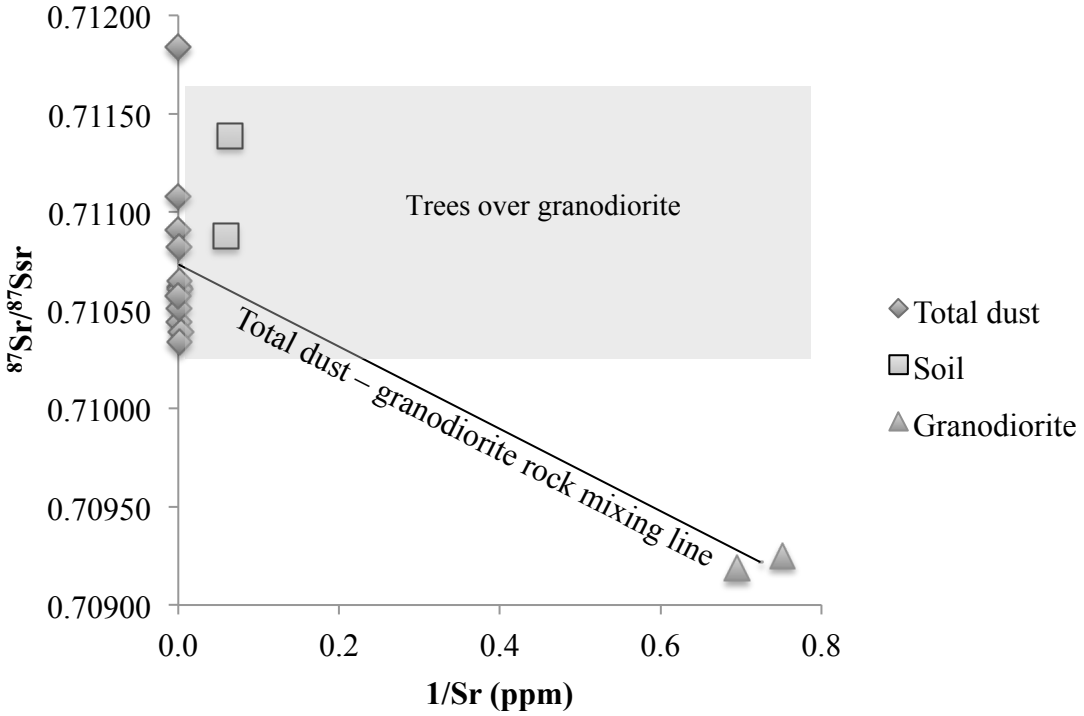

Figure 14. Granodiorite system. Mixing of total dust (water and acid soluble fraction) and granodiorite bedrock, soil over granodiorite, and trees growing over granodiorite. Tree data are the average and range of $^{87}Sr/^{86}Sr$ ratios of trees growing over granodiorite.

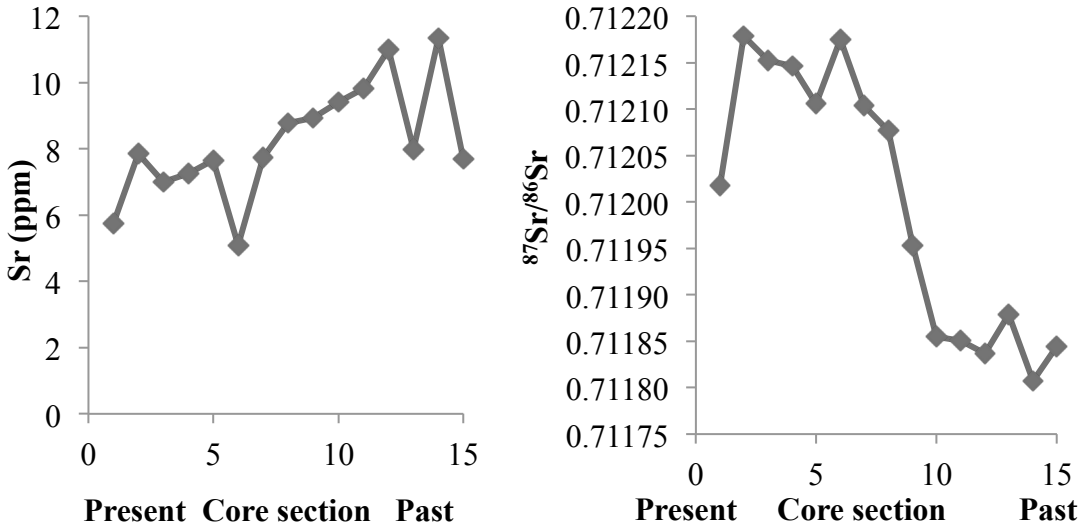

Figure 15. Strontium changes in a tree core over time. Core section 1 = outermost ring, present day. Core section 15 = innermost ring, roughly 75 years ago.

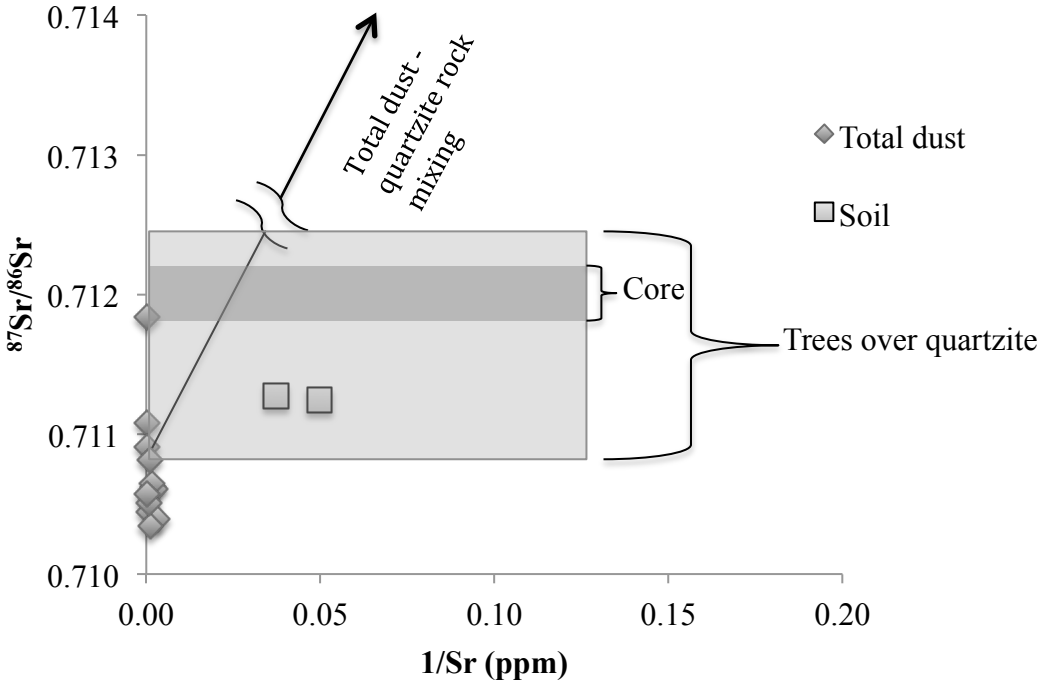

Figure 16. Quartzite soils, total dust, all trees growing over quartzite, and tree used for chronology. Core data are average and range of all core $^{87}Sr/^{86}Sr$ ratios. Tree data are average and range of all trees growing over quartzite $^{87}Sr/^{86}Sr$ ratios. Core $^{87}Sr/^{86}Sr$ ratios back in time are within range of all trees over quartzite $^{87}Sr/^{86}Sr$ ratios, and close to total dust $^{87}Sr/^{86}Sr$ ratios.

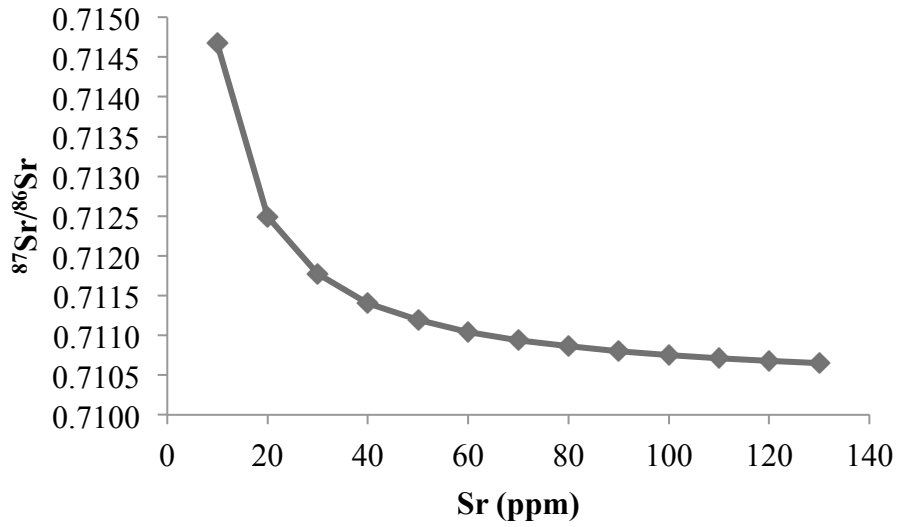

Figure 17. Sensitivity of mixing model to changes in concentration. Predicted dust $^{87}Sr/^{86}Sr$ ratios for a range of input dust strontium concentrations using a two-component mixing model that considers trees growing over quartzite, total dust, and quartzite.

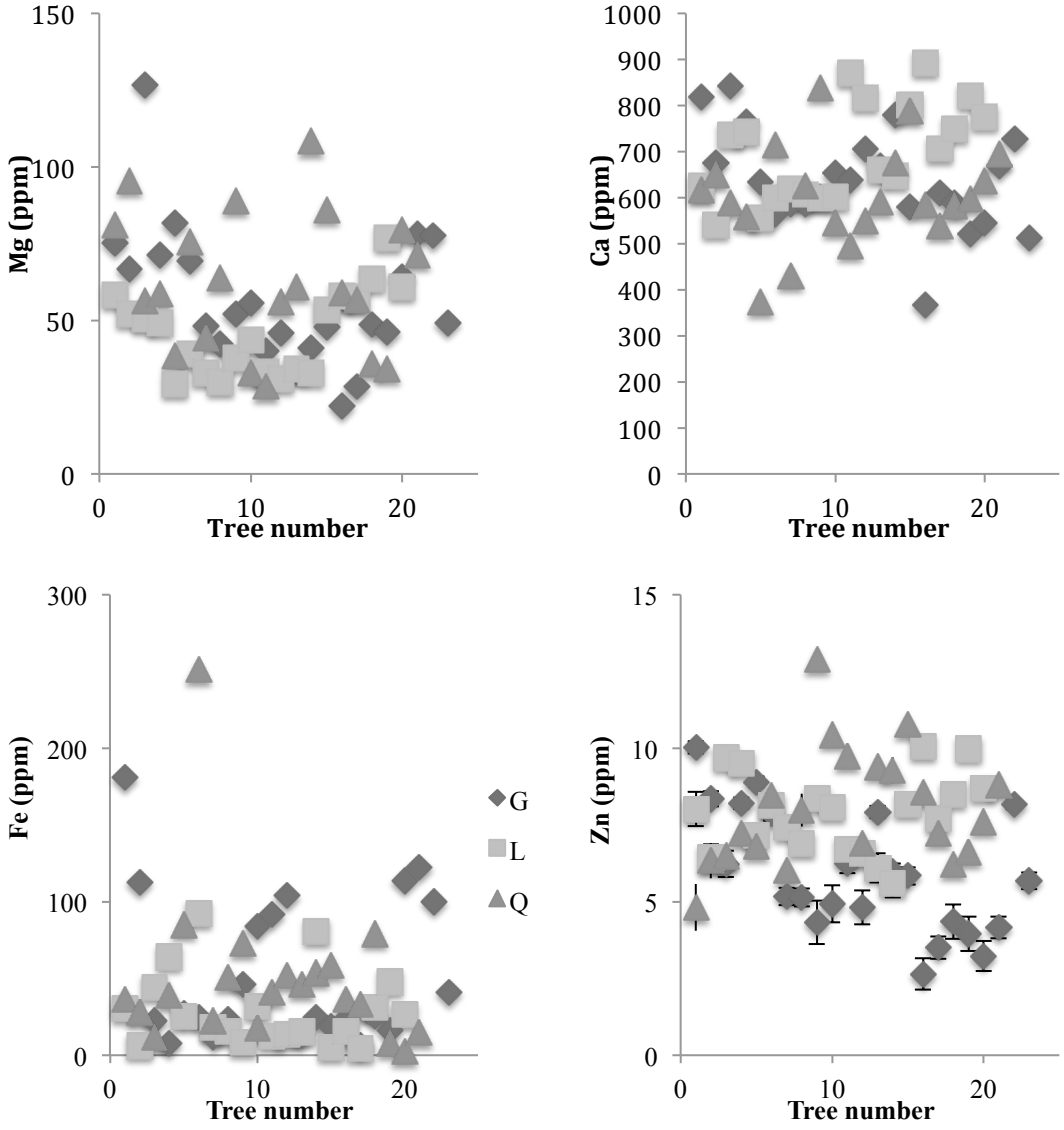

Figure 18. Elements that do not vary by bedrock type in tree tissue. Concentrations of zinc, magnesium, iron, and calcium in tree rings from trees grown on different bedrock types do not vary by bedrock type. G = tree growing on granodiorite, L = tree growing on limestone, and Q = tree growing on quartzite.

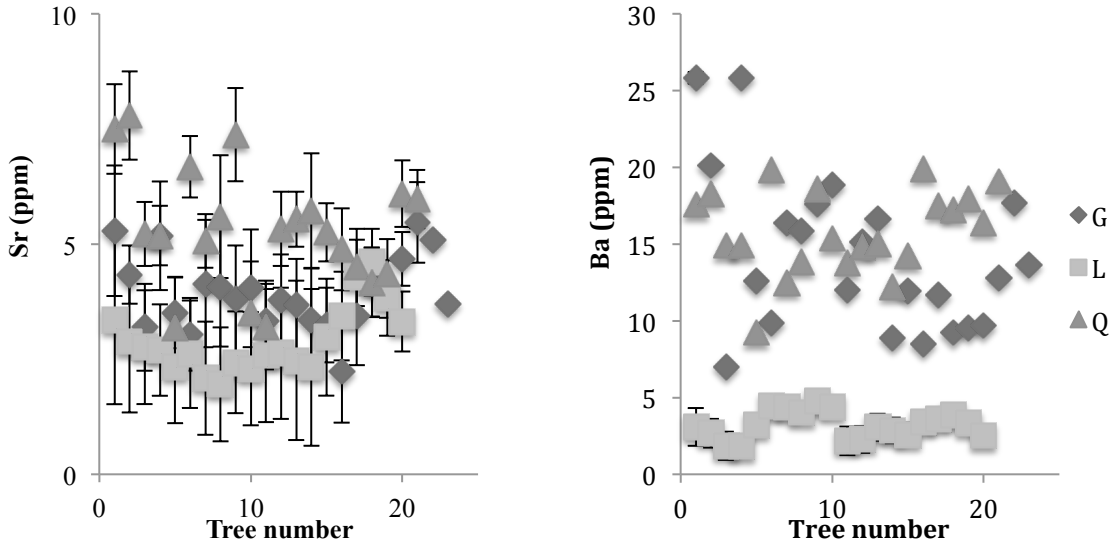

Figure 19. Elements that do vary by bedrock type in tree tissue. Strontium and barium concentrations in woody tissue vary by bedrock type. G = tree growing on granodiorite, L = tree growing on limestone, and Q = tree growing on quartzite.

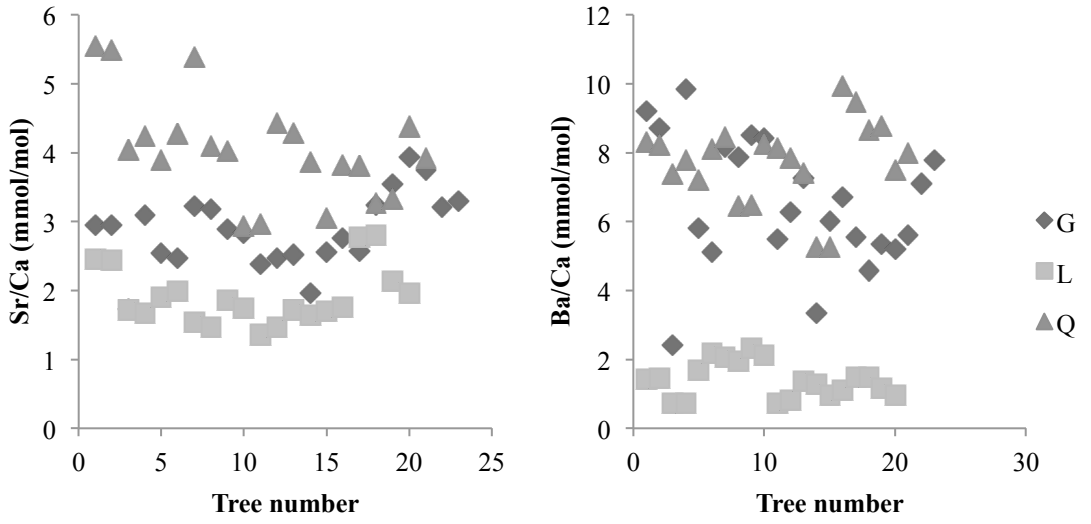

Figure 20. Sr/Ca and Ba/Ca ratios show bedrock dependency. G = tree growing on granodiorite, L = tree growing on limestone, and Q = tree growing on quartzite.

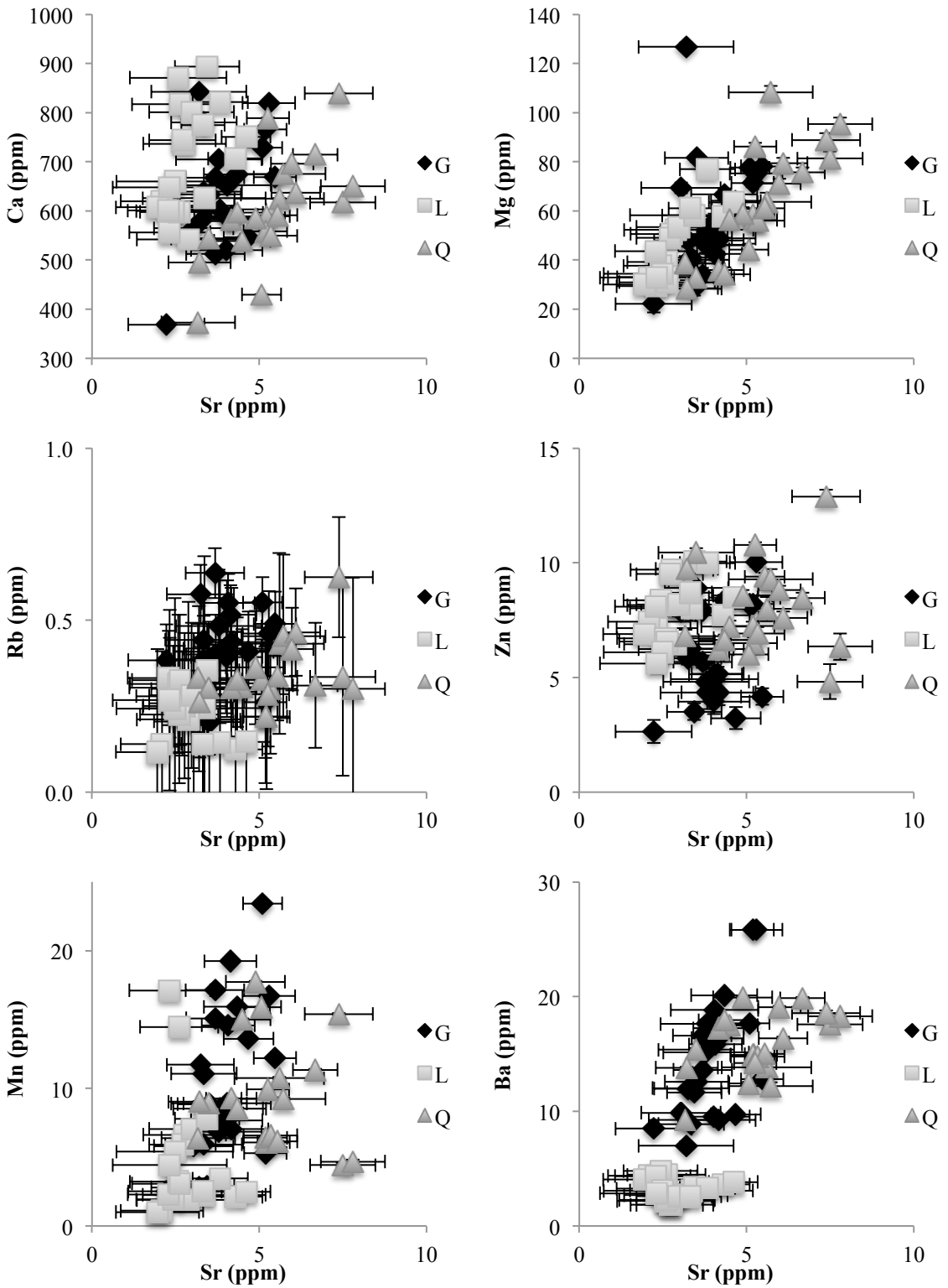

Figure 21. Elements in comparison to strontium that vary by bedrock type. Some elements, such as Ca, Mg, Rb, Zn, Mn, and Ba, in comparison to Sr, show zones based on the bedrock type the trees grew on.

DISCUSSION

Dust events and chemistry

Pinpointing dust source areas is a complex problem. Simple satellite imagery analysis can yield limited information. While MODIS images may show one main plume, other active dust plumes may not be identifiable via MODIS images. Additionally, multiple plumes may be activated at one time and may mix in the atmosphere during transport, and one source area may become more dominant chemically. Cloud cover can make it impossible to identify dust. Additionally, the satellites pass over Utah in the early afternoon, and while this is a common time for dust transport, if the event occurs while the satellite is out of range, it will not be recorded in the satellite image. Sophisticated algorithms may be applied to pinpoint sources (Steenburgh et al., 2012), although this was outside of the scope of this thesis. While source identification is useful from a land management perspective, dust sources will change over time and so a more holistic approach to land management must be used, considering future as well as current and past land uses in mitigating dust production. Regardless of the difficulty of identifying specific sources, the chemistry of dust that is deposited on the Wasatch Mountains is actually more important as this is the dust that will enter the biogeochemical cycle.

The dry 2011-2012 winter had a few effects on dust events, and dust sampling. Dust events occur mainly in the spring. However, the snowpack had already started to

melt by the time of peak dust deposition. This resulted in a sampling bias towards winter dust events that may not represent the more typical dust event. Dust samples were not collected after snowmelt began because older dust layers began to be revealed as the snow melted, and so dust layers were mixed together. Additionally, vertical transport and contamination between layers facilitated by water movement within the snowpack was avoided.

Specific dust events tend to cluster around a specific strontium isotope signature. There was, however, significant temporal variability that indicates that within one winter, there was variation in the source of dust deposited on the Wasatch Mountains.

There was some spatial variability in dust $^{87}Sr/^{86}Sr$ ratio as well. The Mill Creek Canyon site had a different $^{87}Sr/^{86}Sr$ ratio than the Little Cottonwood Canyon and Big Cottonwood Canyon site for several events (D2, D3, and D4). This could represent spatial variability in dust deposition. The Mill Creek Canyon site is further north than the two other sites, and is farther away than both the Big Cottonwood Canyon site and the Little Cottonwood Canyon site are from each other. Another explanation is that the dust from the Mill Creek Canyon site remained in the snowpack for a longer period of time than the dust at the Big and Little Cottonwood Canyon sites. Dust samples were collected from these two sites sooner after deposition than at the Mill Creek Canyon sites. However, to achieve the significantly different $^{87}Sr/^{86}Sr$ ratios observed, the dust would have to mix with another substance that had very different $^{87}Sr/^{86}Sr$ ratios and given the cold snowpack, there doesn't seem to be a mechanism for this mixing to occur. A third possibility is that additional deposition from different sources was occurring at the Mill Creek Canyon site. This site is closer to a freeway than the other two sites, as well as the

Great Salt Lake (Table 3), which has been proven as a major source for ion deposition to the snowpack (Arens, 2010).

Sources of strontium and other elements for trees and soil

The strontium isotopic ratios of tree rings indicate that trees growing on different rock types get their strontium from different sources, although the dominant source of strontium is dust. Trees growing on limestone may not get as much strontium from dust because the limestone is an easily weathered source of abundant calcium and strontium that may overwhelm the dust signal. There was no observed association between soil depth and strontium source for the trees growing over limestone that sourced their strontium from dust. Trees growing on limestone outcrops and trees with thick soils both fall into the group that sources their strontium from dust. The wide range of possible percentages of strontium from dust in trees over granodiorite is a result of a high degree of variation among the samples within the granodiorite system. However, trees growing on granodiorite may get most of their strontium from dust because the dust is a more easily weathered, bioavailable source of strontium than the granodiorite. Additionally, the granodiorite does not contain very much strontium.

Interestingly, while soil formed over limestone had the highest concentration of strontium, woody tissue from trees growing on limestone bedrock had some of the lowest strontium concentrations. Soil over quartzite had the next highest abundance of strontium followed by soil over granodiorite, while for woody tissue, trees growing on quartzite had the most strontium, followed by trees growing on granodiorite (tree Sr: quartzite>granodiorite>limestone, soil Sr: limestone>quartzite>granodiorite). While

limestone rock was not analyzed, quartzite has slightly more strontium than granodiorite, which follows the soil trend. Perhaps the high abundance of strontium in soils over limestone, from both dust and weathered limestone, allows for vegetation to be more selective about strontium uptake than trees growing in soils with lower strontium concentrations.

Trees growing on quartzite may get most of their strontium from dust because there is very little strontium in quartzite. Trees growing on quartzite and granodiorite will be more useful than trees growing on limestone for observing changes in dust sources because the trees growing on limestone get less of their strontium from dust. However, to reliably use a tree growing over granodiorite, more extensive sample analysis is required to determine strontium concentrations and $^{87}Sr/^{86}Sr$ ratios of the bedrock and soil.

Further, the observation that there is little difference between the $^{87}Sr/^{86}Sr$ ratios of two cores from the same tree indicates that the tree rings are a sensitive biomarker for strontium and that changes in the strontium source will appear in the tree rings. The larger variation in concentration, however, can make quantifying strontium source more difficult using two end member isotope mixing models. It also raises the question of what strontium concentration is appropriate to use to determine dust and bedrock contributions to trees. The elemental characterization of soil and bedrock samples, while limited by a small number of samples, still lends itself to a basic understanding of the system and elemental pools.

The strontium available to vegetation in the soil is a mixture of water and acid-soluble fractions of dust as well as the underlying bedrock. This end product of the dust deposition on snow, partial dissolution, and incorporation into soil, is what the vegetation

ultimately has available for it to draw from. Soils, regardless of bedrock type, are strongly affected by dust deposition. Dust can have a relatively influential role in soil formation at this sample site perhaps due to the shallow nature of the soils. While bedrock does have some influence, mixing models show that 85-100% of the strontium in trees growing over quartzite is from dust, 54 to 100% of strontium in trees growing over granodiorite is from dust, and 24 to 97% of strontium in trees growing over limestone is from dust. Dust is the more significant source of strontium in all soils as well. While limestone may be able to contribute more strontium to the overlying soils and trees than other bedrock types, dust is still the major source. Despite the range of possibilities, the similarity of the $^{87}Sr/^{86}Sr$ ratios suggests that trees record a dust signal and can be used to trace dust deposition through time in tree rings. Strontium from dust is the major source of strontium in soils and trees over all three bedrock types.

In terms of element uptake, trees get some of their elements from different sources as well. Many elements in tree material do not vary by bedrock type, including zinc, magnesium, iron, and calcium. However, strontium, barium, Sr/Ca and Ba/Ca ratios, do vary by bedrock type. Additionally, some elements, such as magnesium, rubidium, zinc, manganese, and barium, in comparison with strontium, do reveal bedrock-dependent patterns. This indicates that bedrock is certainly influential in vegetative nutrient uptake, and that elemental sources vary. While this study does not have the data to show that certain elements in tree rings are from dust, the variation for some elements and lack of variation for others suggests that dust may be a factor. Additionally, certain biological processes may regulate the amount of certain elements that accumulate within the woody tissue.

Notably, calcium concentration in tree tissue does not vary by bedrock type. This is surprising given that while strontium substitutes for calcium in mineral lattices, strontium concentration does vary by bedrock type. Calcium is an essential element for trees, and is used in living cells while strontium is nonessential. Perhaps there is less calcium concentration variability across bedrock types because calcium concentration is a function of the trees' necessity for the element, while there is greater variation in strontium concentration because strontium concentration is a function of availability. Further, when coupled with $^{87}Sr/^{86}Sr$ ratios, strontium proves itself a useful tracer of bedrock influence in tree tissue. Overall, elemental results echo the strontium results, indicating that trees get their nutrients from different sources, depending on bedrock. Note that the source change does not necessarily parallel the bedrock change. Certain bedrocks allow dust to be a more significant source of nutrients for vegetation.

Strontium chronology in a tree core

In the core used to develop a dust chronology, the $^{87}Sr/^{86}Sr$ ratios and strontium concentrations change over time. Ratios of $^{87}Sr/^{86}Sr$ increase while abundance of strontium decreases. The changes are nearly sequential. There is also a significant shift in the strontium signature that occurs halfway through the tree's life, where the tree shifts its source of strontium. Although some of this could be due to growth of the tree, and the development of deeper roots that could source strontium from weathered bedrock more readily, the overall shift is small enough that the dominant source of strontium still seems to be dust. Because the shift is within the dust range, this can be interpreted as the tree recording changes in dust sources. Additionally, magnesium, calcium, manganese,

barium, and zinc concentrations follow the same decreasing trend as strontium, suggesting that they are also sourced from dust.

Ideally, the measured strontium in the tree rings could be used to calculate the $^{87}Sr/^{86}Sr$ ratio of dust back in time. However, this requires a good understanding of the dust strontium concentration back in time. The strontium concentration in the tree varies back in time, and so there is no way to know the dust strontium concentration. Additionally, the mixing model used to predict $^{87}Sr/^{86}Sr$ ratios is very sensitive to changes in strontium concentration, particularly over the range of concentrations in dust used in this study, which can be taken as generally representative of the average dust flux.

One way to get around these issues is to test the slope of the strontium over time in multiple cores growing over multiple bedrock types. A parallel trend, regardless of bedrock type would indicate that the changes are due to changes in dust over time. A bedrock dependent trend, where each tree moves closer to its bedrock source would indicate that the tree is changing strontium sources throughout its lifetime from more dust as a young tree to more bedrock as the tree ages. These are valid conclusions if we assume that the soil solution is at calcite saturation, and that the uptake rate of strontium by trees has been constant over time. These assumptions result in a constant input from bedrock weathering over time, making any changes in the strontium in trees due to changes in dust.

Study issues

This study did not attempt to quantify the strontium inputs from precipitation or groundwater $^{87}Sr/^{86}Sr$ ratios, nor did it asses canopy impaction. Some of the difference between the calculated mixed isotopic ratio and the measured isotopic ratio could be due to these processes. Ignoring the impact of canopy impaction would result in an underestimation of the nutrient conservative ability of an ecosystem and an overestimation of the soil weathering process (Gosz et al., 1983).

The low concentration of strontium in some dust samples makes it more difficult to measure accurate strontium isotopic ratios. Matrix effects can also make accurate measurements more difficult, although much of this is removed using the SrFast method. Error estimates on elemental concentrations include interpolation error on the calibration curve, error on the blank measurement, measurement error, and weighing errors. Errors on $^{87}Sr/^{86}Sr$ ratios include the standard error on the measurement.

There are several shortcomings of this project. Certainly, this study would benefit from a more thorough analysis of soil and rock samples. Expanding the sample set would allow for a more complete understanding of this system. Additionally, leaching dust with acetic acid instead of the cold leach would mimic the natural system better. However, this would have reduced the ability to compare dust deposited on the Wasatch Mountains with source soils. Laboratory tests show that the cold leach produces a lower $^{87}Sr/^{86}Sr$ ratio than the acetic acid leach, which would actually place the dust above all soils and granodiorite bedrock. For the quartzite system, this leaves no source for the lower $^{87}Sr/^{86}Sr$ ratios of the soil and trees, depending on the magnitude of the isotopic shift. The soil values are actually the lower limit of the $^{87}Sr/^{86}Sr$ ratios of the dust because the

bedrock values are higher. However, due to the low number of soil samples, the dust range presented above is an appropriate first order assessment. If the shift was not that significant, then it would actually indicate that more of the strontium in the trees was from dust.

More dust samples over time would also add to a deeper understanding of the strontium isotopic signal of dust deposited on the Wasatch Mountains. The samples for this study were taken over an unusual winter in meteorological terms, and this could bias the study towards certain dust source that may not be the most common. It would also bias the study towards winter dust events, and not the more typical spring dust events.

Table 3. Distances from sample sites to the Great Salt Lake and nearest freeway.

Site	Distance to Great Salt Lake (km)	Distance to nearest freeway (km)
Little Cottonwood Canyon	51	24
Big Cottonwood Canyon	53	27
Mill Creek Canyon	47	8

CONCLUSION

Strontium isotopes have shed light on many of the complexities of biogeochemical processes. At the intersection of the Basin and Range province and the Rocky Mountain province, they have proven themselves as an incredibly useful tracer of biogeochemical processes, such as dust transport, soil formation and evolution, nutrient cycling, weathering, and ecological changes. They have provided ample evidence that atmospheric input is a very important component of soil and source of vegetation nutrients.

From the evidence presented above, dust originating in the Sevier Desert is transported to the Wasatch Mountains, where is can be deposited on the snowpack. As the snowpack melts, this dust is incorporated into the underlying soil, and becomes a major source of some nutrients, including strontium, for vegetation. Most of the strontium in soils and trees comes from dust. Trees incorporate the strontium into their woody tissue, all the while retaining the initial $^{87}Sr/^{86}Sr$ ratio of the deposited dust. While strontium concentrations display greater natural heterogeneity, isotopes reveal distinct patterns, and thus lend themselves as a tool for developing a deeper understanding of the strontium cycle.

Each year this cycle occurs, and the tree grows a new annual ring that reflects the strontium isotopic signature of that winter's dust. As certain dust sources are more significant than others, and as dust sources change, over time, the trees seem to record

these changes. Over time, the tree core analyzed in this study had a slight change in strontium source. Strontium abundances and $^{87}Sr/^{86}Sr$ ratios changed, indicating a source change halfway through the tree's life. This source change is still within the dust source range of $^{87}Sr/^{86}Sr$ ratios, indicating that the source of the dust has shifted. Additionally, sequential changes over the life of the tree are punctuated by significant departures from the overall trend, which could coincide with unusual dust events or annul shifts.

APPENDIX

Table 4. Elements in tree rings. Elemental results of woody tissue from tree ring sections in trees growing on different rock types. G = tree over granodiorite, L = tree over limestone, and Q = tree over quartzite. A and B indicate upper and lower core taken 10 cm apart from the same tree. The uncertainty is based on a standard uncertainty multiplied by a coverage factor *k*=2, providing a level of confidence of approximately 95%.

Sample	Mg ppm	Uncertainty	K ppm	Uncertainty	Ca ppm	Uncertainty
G10A	75	2	278.6	0.5	819.4	0.5
G10B	67	2	204.6	0.6	674.4	0.6
G1A	127	2	206.9	0.8	842.4	0.7
G1B	71	2	189.2	0.5	765.6	0.4
G2A	82	2	170.3	0.6	633.2	0.5
G2B	69	2	177.4	0.6	564.5	0.7
G3A	48	2	172.3	0.6	586.1	0.5
G3B	43	3	183.4	0.5	585.4	0.6
G4A	52	3	126	1	603	1
G4B	56	3	133	1	652.7	0.9
G5A	40	3	137.0	0.9	639.5	0.7
G5B	46	3	163.2	0.9	705.2	0.8
G6 East	34	3	193.7	0.5	667.6	0.5
G6 North	41	3	139.1	0.7	779.8	0.5
G6 West	48	3	193.9	0.6	578.8	0.6
G6A South	22	3	125.3	0.7	368.4	0.7
G6B South	28	3	102.3	0.7	610.9	0.5
G7A	49	3	250.0	0.6	589.3	0.8
G7B	46	3	212.1	0.6	520.5	0.8
G8A	64	2	124.6	0.7	545.9	0.6
G8B	78	2	146.5	0.6	668.5	0.5
G9A	78	1	238.5	0.4	728.4	0.4
G9B	49	2	163.7	0.6	512.1	0.6
L10A	58	4	283.6	0.8	626	1

Table 4 continued

Sample	Mg ppm	Uncertainty	K ppm	Uncertainty	Ca ppm	Uncertainty
L10B	52	3	249.4	0.7	541.7	0.9
L1A	51	3	192.3	0.6	736.4	0.5
L1B	49	2	193.0	0.5	743.6	0.4
L2A	29	3	124.2	0.8	556.2	0.6
L2B	39	3	102.7	0.9	598.0	0.6
L3A	33	3	123.9	0.7	619.6	0.5
L3B	30	3	111.2	0.7	607.1	0.5
L4A	38	3	283.5	0.3	599.8	0.5
L4B	44	2	350.5	0.3	600.8	0.5
L5A	33	3	125.5	0.9	871.2	0.5
L5B	31	4	111	1	816.8	0.6
L6A	34	4	125	1	659.5	0.8
L6B	33	4	121	1	647.6	0.8
L7A	53	3	188.6	0.7	800.9	0.6
L7B	58	2	228.9	0.5	893.3	0.4
L8A	58	2	140.7	0.7	706.5	0.5
L8B	63	2	156.3	0.6	750.6	0.5
L9A	77	2	105.0	0.8	821.1	0.4
L9B	61	1	111.2	0.5	774.7	0.3
Q11A	81	3	317.5	0.7	617	1
Q11B	95	3	325.4	0.7	651	1
Q1A	56	2	163.4	0.6	589.1	0.6
Q1B	59	2	163.1	0.6	558.9	0.6
Q2A	38	3	223.1	0.5	372.9	0.9
Q2AX	76	2	232.3	0.6	714.4	0.6
Q2B	44	2	210.2	0.4	429.9	0.6
Q3A	64	4	243	1.0	625	1
Q3B	89	3	396.2	0.6	839.2	0.8
Q4A	33	4	191.7	0.7	543.8	0.8
Q4B	29	3	163.3	0.6	495.3	0.6
Q5A	56	3	174.8	0.7	549.2	0.7
Q5B	61	2	199.1	0.5	591.5	0.5
Q6A	108	3	334.4	0.7	675	1
Q6B	86	2	207.3	0.5	789.1	0.4
Q7A	59	3	226.7	0.6	584.9	0.7
Q7B	57	2	188.4	0.6	538.9	0.7
Q8A	36	3	161.3	0.6	582.0	0.5
Q8B	34	3	177.4	0.6	596.5	0.6

Table 4 continued

Sample	Mg ppm	Uncertainty	K ppm	Uncertainty	Ca ppm	Uncertainty
Q9A	**79**	**2**	**187.0**	**0.7**	**636.7**	**0.7**
Q9B	**71**	**2**	**170.1**	**0.6**	**696.5**	**0.5**

Sample	Mn ppm	Uncertainty	Fe ppm	Uncertainty	Zn ppm	Uncertainty
G10A	16.7	0.1	180.6	0.1	10.0	0.2
G10B	15.9	0.05	112.7	0.1	8.4	0.3
G1A	2.8	0.2	22.4	0.4	6.2	0.4
G1B	5.3	0.1	7.9	0.6	8.2	0.2
G2A	8.8	0.1	27.4	0.2	8.9	0.2
G2B	5.8	0.1	24.6	0.2	7.9	0.2
G3A	19.2	0.04	11.8	0.4	5.2	0.3
G3B	14.6	0.04	23.3	0.2	5.1	0.3
G4A	8.5	0.1	46.0	0.2	4.3	0.7
G4B	8.9	0.1	84.0	0.1	4.9	0.6
G5A	5.9	0.1	91.6	0.1	6.3	0.3
G5B	6.8	0.1	104.1	0.1	4.8	0.6
G6 East	17.1	0.1	13.0	0.4	7.9	0.2
G6 North	11.1	0.05	24.3	0.2	6.0	0.3
G6 West	11.7	0.05	18.8	0.3	5.8	0.3
G6A South	2.5	0.1	23.4	0.2	2.6	0.5
G6B South	2.9	0.1	6.2	0.6	3.5	0.4
G7A	7.0	0.1	25.3	0.3	4.3	0.6
G7B	7.7	0.1	16.2	0.4	4.0	0.6
G8A	13.6	0.04	113.6	0.1	3.2	0.5
G8B	12.2	0.04	122.4	0.1	4.2	0.4
G9A	23.4	0.04	99.7	0.1	8.2	0.2
G9B	15.1	0.04	41.1	0.1	5.7	0.3
L10A	2.3	0.4	30.8	0.4	8.0	0.6
L10B	1.9	0.3	6.0	1.1	6.5	0.4
L1A	6.6	0.1	44.6	0.1	9.7	0.2
L1B	5.9	0.1	63.9	0.1	9.5	0.1
L2A	17.1	0.1	25.4	0.2	7.2	0.2
L2B	14.5	0.04	92.3	0.1	8.2	0.2
L3A	1.1	0.3	18.1	0.3	7.4	0.2

Table 4 continued

Sample	Mn ppm	Uncertainty	Fe ppm	Uncertainty	Zn ppm	Uncertainty
L3B	1.0	0.3	15.5	0.3	6.9	0.2
L4A	1.9	0.2	8.1	0.5	8.4	0.2
L4B	2.3	0.1	31.8	0.2	8.1	0.2
L5A	3.2	0.1	12.2	0.5	6.7	0.3
L5B	3.1	0.2	13.5	0.5	6.6	0.3
L6A	5.4	0.1	15.2	0.5	6.1	0.5
L6B	4.4	0.1	80.6	0.1	5.6	0.5
L7A	7.0	0.1	5	1	8.2	0.3
L7B	7.8	0.1	15.5	0.3	10.1	0.2
L8A	2.1	0.2	4.3	0.9	7.7	0.2
L8B	2.5	0.1	31.1	0.2	8.5	0.2
L9A	3.4	0.1	47.9	0.1	10.0	0.2
L9B	2.5	0.1	26.5	0.1	8.7	0.1
Q11A	4.4	0.2	36.3	0.3	4.8	0.8
Q11B	4.7	0.2	28.2	0.4	6.3	0.6
Q1A	6.1	0.1	11.4	0.5	6.5	0.3
Q1B	6.4	0.1	39.1	0.1	7.2	0.2
Q2A	6.4	0.1	84.7	0.1	6.8	0.3
Q2AX	11.3	0.1	251.3	0.1	8.5	0.2
Q2B	15.9	0.04	22.5	0.2	6.0	0.2
Q3A	10.7	0.1	50.7	0.3	8.0	0.5
Q3B	15.4	0.1	72.7	0.2	12.9	0.3
Q4A	8.9	0.1	17.8	0.4	10.4	0.2
Q4B	9.0	0.1	41.1	0.1	9.7	0.2
Q5A	6.6	0.1	51.9	0.1	6.9	0.3
Q5B	6.1	0.1	45.9	0.1	9.4	0.2
Q6A	9.2	0.1	53.8	0.2	9.3	0.4
Q6B	9.9	0.04	58.5	0.1	10.8	0.1
Q7A	17.7	0.05	36.5	0.2	8.6	0.2
Q7B	15.0	0.05	33.1	0.2	7.2	0.2
Q8A	9.3	0.1	78.9	0.1	6.2	0.2
Q8B	8.5	0.1	7.9	0.6	6.6	0.2
Q9A	36.5	0.1	3	2	7.6	0.3
Q9B	32.6	0.04	14.9	0.4	8.8	0.2

Table 4 continued

Sample	Rb ppm	Uncertainty	Ba ppm	Uncertainty
G10A	0.5	0.1	25.8	0.1
G10B	0.3	0.2	20.1	0.1
G1A	0.3	0.2	7.0	0.4
G1B	0.3	0.2	25.8	0.1
G2A	0.2	0.2	12.6	0.1
G2B	0.2	0.3	9.9	0.2
G3A	0.5	0.1	16.4	0.1
G3B	0.5	0.1	15.8	0.1
G4A	0.4	0.2	17.6	0.2
G4B	0.4	0.2	18.8	0.2
G5A	0.4	0.1	12.0	0.2
G5B	0.5	0.2	15.1	0.2
G6 East	0.6	0.1	16.6	0.1
G6 North	0.4	0.1	8.9	0.2
G6 West	0.6	0.1	12.0	0.1
G6A South	0.4	0.1	8.5	0.2
G6B South	0.3	0.1	11.6	0.1
G7A	0.4	0.2	9.2	0.3
G7B	0.4	0.2	9.5	0.2
G8A	0.4	0.1	9.7	0.2
G8B	0.5	0.1	12.8	0.1
G9A	0.6	0.1	17.7	0.1
G9B	0.4	0.1	13.6	0.1
L10A	0.2	0.4	3	1
L10B	0.2	0.3	2.7	0.9
L1A	0.3	0.2	1.8	0.9
L1B	0.3	0.2	1.8	0.7
L2A	0.3	0.1	3.2	0.5
L2B	0.2	0.2	4.5	0.4
L3A	0.1	0.3	4.4	0.3
L3B	0.1	0.3	4.0	0.3
L4A	0.3	0.1	4.8	0.3
L4B	0.3	0.1	4.3	0.4
L5A	0.3	0.2	2.2	0.9
L5B	0.3	0.2	2.3	0.9
L6A	0.2	0.3	3.1	0.9
L6B	0.3	0.3	2.8	0.8

Table 4 continued

Sample	Rb ppm	Uncertainty	Ba ppm	Uncertainty
L7A	0.3	0.2	2.6	0.8
L7B	0.4	0.1	3.4	0.5
L8A	0.1	0.3	3.6	0.4
L8B	0.1	0.3	3.8	0.4
L9A	0.1	0.3	3.3	0.4
L9B	0.1	0.2	2.5	0.4
Q11A	0.3	0.3	17.6	0.2
Q11B	0.3	0.3	18.3	0.2
Q1A	0.2	0.2	14.9	0.1
Q1B	0.2	0.2	14.9	0.1
Q2A	0.3	0.2	9.2	0.2
Q2AX	0.3	0.2	19.9	0.1
Q2B	0.3	0.1	12.4	0.1
Q3A	0.4	0.3	13.8	0.3
Q3B	0.6	0.2	18.6	0.2
Q4A	0.3	0.2	15.4	0.1
Q4B	0.3	0.2	13.8	0.1
Q5A	0.3	0.2	14.8	0.1
Q5B	0.3	0.1	15.0	0.1
Q6A	0.5	0.2	12.2	0.3
Q6B	0.3	0.2	14.2	0.1
Q7A	0.4	0.2	19.9	0.1
Q7B	0.3	0.2	17.5	0.1
Q8A	0.3	0.1	17.2	0.1
Q8B	0.3	0.1	18.0	0.1
Q9A	0.5	0.1	16.4	0.1
Q9B	0.4	0.1	19.1	0.1

Sample	Mg/Ca mol/mol	Sr/Ca mmol/mol	Ba/Ca mmol/mol
G10A	0.2	3.0	9.2
G10B	0.2	2.9	8.7
G1A	0.2	1.7	2.4
G1B	0.2	3.1	9.8
G2A	0.2	2.5	5.8
G2B	0.2	2.5	5.1
G3A	0.1	3.2	8.2
G3B	0.1	3.2	7.9

Table 4 continued

Sample	Mg/Ca mol/mol	Sr/Ca mmol/mol	Ba/Ca mmol/mol
G4A	0.1	2.9	8.5
G4B	0.1	2.8	8.4
G5A	0.1	2.4	5.5
G5B	0.1	2.5	6.3
G6 East	0.1	2.5	7.3
G6 North	0.1	2.0	3.3
G6 West	0.1	2.6	6.0
G6A South	0.1	2.8	6.7
G6B South	0.1	2.6	5.6
G7A	0.1	3.2	4.6
G7B	0.1	3.5	5.4
G8A	0.2	3.9	5.2
G8B	0.2	3.7	5.6
G9A	0.2	3.2	7.1
G9B	0.2	3.3	7.8
L10A	0.2	2.5	1.4
L10B	0.2	2.4	1.4
L1A	0.1	1.7	0.7
L1B	0.1	1.7	0.7
L2A	0.1	1.9	1.7
L2B	0.1	2.0	2.2
L3A	0.1	1.5	2.1
L3B	0.1	1.5	1.9
L4A	0.1	1.9	2.3
L4B	0.1	1.7	2.1
L5A	0.1	1.4	0.7
L5B	0.1	1.5	0.8
L6A	0.1	1.7	1.4
L6B	0.1	1.6	1.3
L7A	0.1	1.7	0.9
L7B	0.1	1.8	1.1
L8A	0.1	2.8	1.5
L8B	0.1	2.8	1.5
L9A	0.2	2.1	1.2
L9B	0.1	2.0	1.0
Q11A	0.2	5.5	8.3
Q11B	0.2	5.5	8.2
Q1A	0.2	4.0	7.4
Q1B	0.2	4.2	7.8

Table 4 continued

Sample	Mg/Ca mol/mol	Sr/Ca mmol/mol	Ba/Ca mmol/mol
Q2A	0.2	3.9	7.2
Q2AX	0.2	4.3	8.1
Q2B	0.2	5.4	8.4
Q3A	0.2	4.1	6.4
Q3B	0.2	4.0	6.5
Q4A	0.1	2.9	8.2
Q4B	0.1	3.0	8.1
Q5A	0.2	4.4	7.8
Q5B	0.2	4.3	7.4
Q6A	0.3	3.9	5.3
Q6B	0.2	3.0	5.3
Q7A	0.2	3.8	9.9
Q7B	0.2	3.8	9.5
Q8A	0.1	3.3	8.6
Q8B	0.1	3.3	8.8
Q9A	0.2	4.4	7.5
Q9B	0.2	3.9	8.0

Table 5. Strontium concentration and $^{87}Sr/^{86}Sr$ ratio measurements of tree rings from trees growing over different bedrock types. The uncertainty of the strontium concentration is based on a standard uncertainty multiplied by a coverage factor k=2, providing a level of confidence of approximately 95%. The error on the $^{87}Sr/^{86}Sr$ measurement is the standard error of multiple isotopic ratio measurements.

Sample	Sr ppm	Uncertainty	$^{87}Sr/^{86}Sr$	Measurement standard error
G10A	5.3	0.8	0.71108	0.00001
G10B	4	1	0.71107	0.00002
G1A	3	1	0.71154	0.00002
G1B	5.2	0.6	0.71135	0.00001
G2A	3.5	0.9	0.71164	0.00002
G2B	3	1	0.71161	0.00002
G3A	4.1	0.8	0.71096	0.00001
G3B	4.1	0.8	0.71091	0.00001
G4A	4	1	0.71056	0.00002
G4B	4	1	0.71053	0.00002
G5A	3	1	0.71067	0.00002
G5B	4	1	0.71073	0.00002
G6 East	3.7	0.9	0.71054	0.00021
G6 North	3	1	0.71027	0.00002
G6 West	3	1	0.71092	0.00002
G6A South	2	1	0.71038	0.00002
G6B South	3.4	0.8	0.71025	0.00001
G7A	4	1	0.71052	0.00002
G7B	4	1	0.71049	0.00002
G8A	4.7	0.7	0.71076	0.00001
G8B	5.5	0.6	0.71076	0.00002
G9A	5.1	0.6	0.71090	0.00001
G9B	3.7	0.9	0.71085	0.00002
L10A	3	2	0.70797	0.00290
L10B	3	2	0.70970	0.00002
L1A	3	1	0.70927	0.00002
L1B	3	1	0.70924	0.00002
L2A	2	1	0.70938	0.00002
L2B	3	1	0.70974	0.00002
L3A	2	1	0.71104	0.00002
L3B	2	1	0.71102	0.00002
L4A	2	1	0.71102	0.00002

Table 5 continued

Sample	Sr ppm	Uncertainty	$^{87}Sr/^{86}Sr$	Measurement standard error
L4B	2	1	0.71090	0.00002
L5A	3	1	0.70927	0.00002
L5B	3	1	0.70926	0.00002
L6A	2	2	0.70931	0.00002
L6B	2	2	0.70928	0.00002
L7A	3	1	0.70906	0.00001
L7B	3	1	0.70902	0.00002
L8A	4.3	0.8	0.70958	0.00001
L8B	4.6	0.7	0.70959	0.00001
L9A	3.8	0.8	0.71036	0.00001
L9B	3.3	0.6	0.71021	0.00001
Q11A	7	1	0.71187	0.00002
Q11B	8	1	0.71187	0.00002
Q1A	5.2	0.7	0.71218	0.00001
Q1B	5.2	0.6	0.71218	0.00001
Q2A	3	1	0.71198	0.00002
Q2AX	6.7	0.7	0.71209	0.00001
Q2B	5.1	0.6	0.71243	0.00001
Q3A	6	1	0.71226	0.00002
Q3B	7	1	0.71218	0.00002
Q4A	3	1	0.71182	0.00002
Q4B	3.2	0.9	0.71185	0.00002
Q5A	5.3	0.8	0.71216	0.00001
Q5B	5.5	0.6	0.71229	0.00001
Q6A	6	1	0.71163	0.00002
Q6B	5.3	0.6	0.71160	0.00001
Q7A	4.9	0.9	0.71109	0.00002
Q7B	4.5	0.8	0.71111	0.00001
Q8A	4.2	0.8	0.71098	0.00001
Q8B	4.3	0.8	0.71097	0.00001
Q9A	6.1	0.7	0.71081	0.00001
Q9B	6.0	0.6	0.71091	0.00001

Table 6. Elements in tree core over time. Elemental results of tree tissue back in time. C1 is the present, while C15 is the furthest back in time. Sections are made up of five rings. The uncertainty is based on a standard uncertainty multiplied by a coverage factor *k*=2, providing a level of confidence of approximately 95%.

Sample	Na ppm	Uncertainty	Mg ppm	Uncertainty	Al ppm	Uncertainty
C1	8.1	0.3	71.2	0.6	6.3	0.1
C2	7.4	0.3	78.1	0.6	2.3	0.2
C3	4.1	0.5	73.0	0.5	2.1	0.2
C4	3.2	0.5	84.7	0.4	2.6	0.1
C5	4.7	0.5	90.9	0.5	2.2	0.2
C6	~	~	58.7	2.1	~	~
C7	4.2	0.5	85.3	0.4	2.3	0.2
C8	3.5	0.5	99.1	0.3	2.1	0.2
C9	4.1	0.5	102.3	0.4	1.5	0.3
C10	1.9	0.6	103.4	0.2	1.1	0.2
C11	2.9	0.6	114.9	0.3	1.1	0.3
C12	1.9	0.7	110.8	0.2	3.4	0.1
C13	2.6	0.4	88.6	0.3	2.3	0.1
C14	5.0	0.3	128.2	0.3	1.4	0.3
C15	2.5	0.4	73.3	0.3	1.5	0.1
C16	2.3	0.7	121.6	0.3	2.5	0.1

Sample	Ca ppm	Uncertainty	Mn ppm	Uncertainty	Fe ppm	Uncertainty
C1	534.3	0.2	9.08	0.03	130.73	0.03
C2	764.2	0.2	6.80	0.04	55.22	0.04
C3	707.4	0.2	6.15	0.04	42.19	0.04
C4	750.6	0.1	7.44	0.03	81.42	0.03
C5	776.5	0.2	8.42	0.04	66.03	0.04
C6	558.9	0.6	6.4	0.1	39.1	0.1
C7	768.9	0.1	8.76	0.04	25.20	0.06
C8	892.6	0.1	9.12	0.04	21.49	0.06
C9	929.6	0.1	9.37	0.05	9.8	0.1
C10	1014.5	0.1	10.06	0.03	7.2	0.1
C11	1093.6	0.1	11.04	0.03	8.0	0.1
C12	1235.4	0.1	12.40	0.03	19.49	0.06
C13	963.4	0.1	9.65	0.03	3.4	0.2
C14	1393.5	0.1	13.28	0.03	5.8	0.2
C15	1008.2	0.1	7.78	0.03	6.6	0.1
C16	1451.9	0.1	13.09	0.03	15.80	0.07

Table 6 continued

Sample	Cu ppm	Uncertainty	Zn ppm	Uncertainty	Rb ppm	Uncertainty
C1	5.07	0.06	4.71	0.08	0.92	0.05
C2	5.82	0.06	4.78	0.09	0.60	0.07
C3	6.03	0.06	5.80	0.06	0.3	0.1
C4	8.29	0.06	7.38	0.05	0.37	0.08
C5	12.03	0.06	9.18	0.05	0.4	0.1
C6	4.6	0.1	7.2	0.2	0.2	0.4
C7	10.29	0.06	8.02	0.06	0.2	0.1
C8	5.26	0.06	6.54	0.05	0.30	0.09
C9	2.14	0.08	5.23	0.07	0.3	0.1
C10	1.62	0.08	5.67	0.04	0.27	0.08
C11	1.56	0.09	5.81	0.06	0.3	0.1
C12	1.50	0.08	8.28	0.04	0.2	0.1
C13	1.68	0.07	6.57	0.03	0.2	0.1
C14	2.25	0.09	9.06	0.05	0.3	0.1
C15	1.05	0.08	5.54	0.04	0.2	0.1
C16	1.49	0.09	8.82	0.04	0.3	0.1

Sample	Ba ppm	Uncertainty	Pb ppm	Uncertainty
C1	17.38	0.04	0.1	0.1
C2	19.84	0.03	0.1	0.1
C3	18.09	0.03	0.18	0.08
C4	19.14	0.03	0.26	0.08
C5	20.34	0.03	0.38	0.06
C6	14.9	0.1	0.2	0.2
C7	19.77	0.04	0.30	0.06
C8	23.96	0.03	0.1	0.1
C9	26.95	0.03	0.1	0.2
C10	31.34	0.03	0.0	0.2
C11	33.81	0.02	0.0	0.3
C12	41.37	0.03	0.0	0.3
C13	29.55	0.04	0.0	0.2
C14	41.23	0.04	0.1	0.2
C15	25.55	0.03	0.0	0.2
C16	41.59	0.03	0.0	0.3

Table 6 continued

Sample	Mg/Ca mol/mol	Sr/Ca mmol/mol	Ba/Ca mmol/mol
C1	0.22	4.8	9.5
C2	0.17	4.6	7.6
C3	0.17	4.4	7.5
C4	0.19	4.3	7.4
C5	0.19	4.4	7.6
C6		0.17	4.2
C7	0.18	4.5	7.5
C8	0.18	4.4	7.8
C9	0.18	4.3	8.5
C10	0.17	4.2	9.0
C11	0.17	4.0	9.0
C12	0.15	4.0	9.8
C13	0.15	3.7	9.0
C14	0.15	3.7	8.6
C15	0.12	3.4	7.4
C16	0.14	3.9	8.4

Table 7. Strontium concentration and $^{87}Sr/^{86}Sr$ ratio measurements of tree core back in time. The uncertainty of the strontium concentration is based on a standard uncertainty multiplied by a coverage factor k=2, providing a level of confidence of approximately 95%. The error on the $^{87}Sr/^{86}Sr$ measurement is the standard error of multiple isotopic ratio measurements.

Sample	Sr ppm	Uncertainty	$^{87}Sr/^{86}Sr$	Measurement standard error
C1	5.3	0.2	0.71202	0.00001
C2	7.3	0.1	0.71218	0.00001
C3	6.5	0.1	0.71215	0.00002
C4	6.7	0.1	0.71215	0.00002
C5	7.1	0.1	0.71211	0.00002
C6	5.2	0.6	0.71218	0.00001
C7	7.1	0.1	0.71210	0.00001
C8	8.1	0.1	0.71208	0.00002
C9	8.3	0.1	0.71195	0.00001
C10	8.70	0.06	0.71185	0.00002
C11	9.08	0.08	0.71185	0.00001
C12	10.17	0.06	0.71184	0.00002
C13	7.39	0.06	0.71188	0.00002
C14	10.49	0.08	0.71181	0.00002
C15	7.13	0.06	0.71184	0.00002

Table 8. Elemental results for soil and rock samples. G, L, and Q = granodiorite, limestone, and quartzite. S or R = soil or rock. Number indicates site. The uncertainty is based on a standard uncertainty multiplied by a coverage factor *k*=2, providing a level of confidence of approximately 95%.

Sample	Na ppm	Uncertainty	Mg ppm	Uncertainty	Al ppm	Uncertainty
G2S	81.3	0.1	1058.3	0.2	275.36	0.04
G6S	53.8	0.2	507.6	0.5	658.35	0.03
L1S	227.8	0.2	1723.7	0.5	205.7	0.1
L3S	63.2	0.9	2551.2	0.4	202.9	0.1
Q1S	55.9	0.2	591.9	0.4	774.21	0.04
Q11S	180.3	0.1	483.3	0.4	657.89	0.03
Q11R	23.4	0.4	90	1	229.1	0.1
Q1R	35.8	0.3	150	1	453.21	0.04
G2R	48.5	0.2	46	2	210.82	0.05
G6R	39.6	0.3	43	2	248.76	0.04

Sample	Ca ppm	Uncertainty	Ti ppm	Uncertainty	Mn ppm	Uncertainty
G2S	4116.8	0.2	1.1	0.5	260.44	0.03
G6S	3484.4	0.2	0.8	0.8	186.97	0.04
L1S	21487.0	0.1	1	1	241.74	0.04
L3S	66910.9	0.1	1	2	308.18	0.03
Q1S	4150.2	0.2	0.9	0.6	241.08	0.03
Q11S	4684.8	0.1	0.7	0.7	304.91	0.03
Q11R	936.6	0.5	1.0	0.5	10.47	0.07
Q1R	1292.9	0.4	1.6	0.4	11.10	0.06
G2R	471	1	1.7	0.4	17.81	0.07
G6R	511.7	0.9	1.2	0.5	33.96	0.04

Sample	Fe ppm	Uncertainty	Co ppm	Uncertainty	Cu ppm	Uncertainty
G2S	56.5	0.1	1.24	0.09	5.9	0.1
G6S	40.1	0.2	1.0	0.1	4.0	0.2
L1S	30.6	0.9	0.6	0.5	1.2	2.3
L3S	27	1	0.5	0.7	13.4	0.3
Q1S	138.78	0.06	3.71	0.05	7.1	0.1
Q11S	45.8	0.2	2.91	0.04	8.0	0.1

Table 8 continued

Sample	Fe ppm	Uncertainty	Co ppm	Uncertainty	Cu ppm	Uncertainty
Q11R	209.38	0.05	0.1	0.7	1.2	0.7
Q1R	671.36	0.03	0.6	0.2	5.8	0.1
G2R	110.39	0.08	0.6	0.2	1232.43	0.06
G6R	54.0	0.1	0.1	0.6	1	3

Sample	Zn ppm	Uncertainty	Rb ppm	Uncertainty
G2S	16.8	0.1	0.2	0.7
G6S	6.8	0.3	1.0	0.2
L1S	25.7	0.3	0	2
L3S	108.2	0.1	1	1
Q1S	11.4	0.2	0.6	0.3
Q11S	80.39	0.03	0.8	0.2
Q11R	0	2	0.6	0.3
Q1R	1	2	1.5	0.1
G2R	31.86	0.07	0.9	0.2
G6R	0	3	0.5	0.4

Sample	Ba ppm	Uncertainty	Pb ppm	Uncertainty
G2S	56.58	0.05	4.04	0.04
G6S	99.44	0.04	6.57	0.04
L1S	32.6	0.3	19.48	0.04
L3S	43.6	0.3	85.89	0.03
Q1S	62.96	0.05	6.72	0.04
Q11S	73.04	0.04	21.06	0.03
Q11R	12.1	0.2	0	1
Q1R	3.9	0.6	0.1	0.9
G2R	4.4	0.6	2.82	0.05
G6R	9.4	0.3	0.2	0.4

Sample	Mg/Ca mol/mol	Sr/Ca mmol/mol	Ba/Ca mmol/mol
G2S	0.42	1.8	4.0
G6S	0.24	2.4	8.3
L1S	0.13	0.6	0.4

Table 8 continued

Sample	Mg/Ca mol/mol	Sr/Ca mmol/mol	Ba/Ca mmol/mol
L3S	0.06	0.5	0.2
Q1S	0.17	2.8	4.5
Q11S	0.24	2.4	4.4
Q11R	0.19	0.6	0.9
Q1R	0.16	1.3	3.8
G2R	0.16	1.5	2.7
G6R	0.14	1.3	5.4

Table 9. Strontium concentration and $^{87}Sr/^{86}Sr$ ratio measurements of soil and bedrock samples. The uncertainty of the strontium concentration is based on a standard uncertainty multiplied by a coverage factor k=2, providing a level of confidence of approximately 95%. The error on the $^{87}Sr/^{86}Sr$ measurement is the standard error of multiple isotopic ratio measurements.

Sample	Sr ppm	Uncertainty	$^{87}Sr/^{86}$ Sr	Measurement standard error
G2 soil	15.5	0.3	0.71139	0.00002
G6 soil	17.0	0.3	0.71088	0.00001
L1 soil	28.3	0.6	0.71049	0.00002
L3 soil	70.2	0.3	0.71144	0.00002
Q1 soil	20.1	0.2	0.71124	0.00002
Q11 soil	26.9	0.2	0.71127	0.00002
Q11 rock	2	1	0.73719	0.00002
Q1 rock	2	1	0.72182	0.00002
G2 rock	1	2	0.70919	0.00002
G6 rock	1	2	0.70925	0.00002

Table 10. Strontium concentration and $^{87}Sr/^{86}Sr$ isotope ratio in acid and water-soluble fractions of dust. HC = Hidden Canyon, LCC = Little Cottonwood Canyon, MC = Mill Creek Canyon, and b indicated a duplicate sample taken. The uncertainty is based on a standard uncertainty multiplied by a coverage factor *k*=2, providing a level of confidence of approximately 95%.

Event	Dust Sr ppm	Uncertainty	Dust $^{87}Sr/^{86}Sr$	Measurement standard error
HC 2	886	8	0.71157	0.00003
HC 3	15.7	0.4	0.71083	0.00003
HC 3b	236.4	0.7	0.71071	0.00001
HC 4	42.4	0.2	0.71036	0.00001
HC 8	45.5	0.2	0.71032	0.00002
LCC 1	41.5	0.2	0.71037	0.00002
LCC 2	184.3	0.1	0.71180	0.00001
LCC 3	96.0	0.2	0.71078	0.00001
LCC 4	34.9	0.2	0.71061	0.00002
LCC 4b	57.7	0.2	0.71064	0.00001
LCC 8	37.2	0.2	0.71020	0.00002
MC 1	72.7	0.1	0.71033	0.00001
MC 2	174.9	0.2	0.71082	0.00001
MC 3	1573	9	0.71121	0.00001
MC 4	688.8	0.1	0.71236	0.00001
MC 5	111.8	0.2	0.71165	0.00001
MC 6	53.8	0.1	0.71035	0.00001
MC 8	75.6	0.3	0.71033	0.00001

Event	Snowmelt Sr ppm	Uncertainty	Snowmelt $^{87}Sr/^{86}Sr$	Measurement standard error
HC 2	227653	6	0.71195	0.00002
HC 3	4437	7	0.71132	0.00002
HC 3b	15889	7	0.71148	0.00002
HC 4	492	64	0.71088	0.00006
HC 8	350	20	0.71090	0.00004
LCC 1	1263	17	0.71052	0.00003
LCC 2	2736	4	0.71216	0.00002
LCC 3	5540	4	0.71105	0.00002
LCC 4	641	86	0.71068	0.00007
LCC 4b	904	58	0.71100	0.00006
LCC 8	269	8	0.71057	0.00003
MC 1	795	4	0.71034	0.00002

Table 10 continued

Event	Snowmelt Sr ppm	Uncertainty	Snowmelt $^{87}Sr/^{86}Sr$	Measurement standard error
MC 2	4540	3	0.71096	0.00002
MC 3	176437	9	0.71187	0.00002
MC 4	3599	2	0.71217	0.00001
MC 5	4976	3	0.71203	0.00002
MC 6	1276	13	0.71067	0.00003
MC 8	4435	17	0.71081	0.00003

REFERENCES

åberg, G., 1995, The use of natural strontium isotopes as tracers in environmental studies: Water, Air, & Soil Pollution, v. 79, no. 1, p. 309-322.

Amato, I., 1988, Tapping tree rings for the environmental tales they tell: Analytical Chemistry, v. 60, no. 19, p. 1103 A-1107 A.

Arens, S., 2010, Ion deposition in Wasatch Mountain snow: Influence of Great Salt Lake and Salt Lake City [M.S.: University of Utah, 54 p.

Bacardit, M., and Camarero, L., 2010, Atmospherically deposited major and trace elements in the winter snowpack along a gradient of altitude in the Central Pyrenees: The seasonal record of long-range fluxes over SW Europe: Atmospheric Environment, v. 44, no. 4, p. 582-595.

Barnes, D., 1976, The lead, copper and zinc content of tree rings and bark. A measurement of local metallic pollution: Science of The Total Environment, v. 5, no. 1, p. 63-67.

Baruah, B. K., Das, B., Haque, A., Medhi, C., and Misra, A. K., 2011, Sequential extraction of common metals (Na, K, Ca and Mg) from surface soil: Journal of Chemical and Pharmaceutical Research, v. 3, no. 5, p. 565-573.

Belnap, J., and Gillette, D. A., 1997, Disturbance of biological soil crusts: impacts on potential wind erodibility of sandy desert soils in southeastern Utah: Land Degradation & Development, v. 8, no. 4, p. 355-362.

Bryant, B., 1990, Geologic Map of the Salt Lake City 30' x 60' Quadrangle, North-Central Utah, and Uinta County, Wyoming.

Burke, W. H., Denison, R. E., Hetherington, E. A., Koepnick, R. B., Nelson, H. F., and Otto, J. B., 1982, Variation of seawater 87Sr/86Sr throughout Phanerozoic time: Geology, v. 10, no. 10, p. 516-519.

Camberato, J. J., and Pan, W. L., 1999, Bioavailability of Calcium, Magnesium, and Sulfur, *in* Sumner, M. E., ed., Handbook of Soil Science, CRC Press, p. 2148.

Capo, R. C., and Chadwick, O. A., 1999, Sources of strontium and calcium in desert soil and calcrete: Earth and Planetary Science Letters, v. 170, no. 1-2, p. 61-72.

Capo, R. C., Stewart, B. W., and Chadwick, O. A., 1998, Strontium isotopes as tracers of ecosystem processes: Theory and methods: Geoderma, v. 82, no. 1–3, p. 197-225.

Carling, G. T., Fernandez, D. P., and Johnson, W. P., 2012, Dust-mediated loading of trace and major elements to Wasatch Mountain snowpack: Science of the Total Environment, v. 432, no. 0, p. 65-77.

Center, N. N. C. D., 2012, State of the Climate: National Snow & Ice for Annual 2012.

Chen, L., Wu, F. H., Liu, T. W., Chen, J., Li, Z. J., Pei, Z. M., and Zheng, H. L., 2010, Soil acidity reconstruction based on tree ring information of a dominant species Abies fabri in the subalpine forest ecosystems in southwest China: Environmental Pollution, v. 158, no. 10, p. 3219-3224.

Chiquet, A., Michard, A., Nahon, D., and Hamelin, B., 1999, Atmospheric input vs in situ weathering in the genesis of calcretes: An Sr isotope study at Galvez (Central Spain): Geochimica et Cosmochimica Acta, v. 63, no. 3-4, p. 311-323.

Conway, H., Gades, A., and Raymond, C. F., 1996, Albedo of dirty snow during conditions of melt: Water Resour. Res., v. 32, no. 6, p. 1713-1718.

Cutter, B. E., and Guyette, R. P., 1993, Anatomical, Chemical, And Ecological Factors Affecting Tree Species Choice In Dendrochemistry Studies: J. Environ. Qual., v. 22, no. 3, p. 611-619.

Dart, R. C., Wittwer, P. D., Barovich, K. M., Chittleborough, D. J., and Hill, S. M., 2004, Strontium isotopes as an indicator of the source of calcium for regolith carbonates, *in* Roach, I. C., ed., Regolith: Adelaide, South Australia, CRC LEME, p. 67-70.

Donnelly, J. R., Shane, J. B., and Schaberg, P. G., 1990, Lead mobility within the xylem of red spruce seedlings: Implications for the development of pollution histories: Journal of Environmental Quality, v. 19, no. 2, p. 268-271.

Draxler, R. R., and Rolph, G. D., 2012, HYSPLIT (HYbrid Single-Particle Lagrangian Integrated Trajectory), Volume 2012: Model access via NOAA ARL READY Website (http://ready.arl.noaa.gov/HYSPLIT.php), NOAA Air Resources Laboratory, Silver Spring, MD.

Edmond, J. M., 1992, Himalayan tectonics, weathering processes, and the strontium isotope record in marine limestones: Science, v. 258, no. 5088, p. 1594-1597.

Eghbal, M. K., 1993, Stratigraphy and genesis of Durorthids and Haplargids on dissected alluvial fans, western Mojave Desert, California: Geoderma, v. 59, no. 1-4, p. 151-174.

Eldridge, D. J., and Leys, J. F., 2003, Exploring some relationships between biological soil crusts, soil aggregation and wind erosion: Journal of Arid Environments, v. 53, no. 4, p. 457-466.

English, N. B., Betancourt, J. L., Dean, J. S., and Quade, J., 2001, Strontium isotopes reveal distant sources of architectural timber in Chaco Canyon, New Mexico: Proceedings of the National Academy of Sciences.

Faure, G., 1977, Strontium isotope geology, John Wiley and Sons, Inc.,New York, NY.

Field, J. P., Belnap, J., Breshears, D. D., Neff, J. C., Okin, G. S., Whicker, J. J., Painter, T. H., Ravi, S., Reheis, M. C., and Reynolds, R. L., 2009a, The ecology of dust: Frontiers in Ecology and the Environment, v. 8, no. 8, p. 423-430.

Field, J. P., Breshears, D. D., and Whicker, J. J., 2009b, Toward a more holistic perspective of soil erosion: Why aeolian research needs to explicitly consider fluvial processes and interactions: Aeolian Research, v. 1, no. 1–2, p. 9-17.

Gerloff, G. C., Moore, D. G., and Curtis, J. T., 1966, Selective absorption of mineral elements by native plants of Wisconsin: Plant and Soil, v. 25, no. 3, p. 393-405.

Gosz, J. R., Brookins, D. G., and Moore, D. I., 1983, Using strontium isotope ratios to estimate inputs to ecosystems: BioScience, v. 33, no. 1, p. 23-30.

Graustein, W. C., and Armstrong, R. L., 1983, The use of strontium-87/strontium-86 ratios to measure atmospheric transport into forested watersheds: Science, v. 219, no. 4582, p. 289-292.

Grousset, F. E., and Biscaye, P. E., 2005, Tracing dust sources and transport patterns using Sr, Nd and Pb isotopes: Chemical Geology, v. 222, no. 3–4, p. 149-167.

Hagemeyer, J., 2000, Chapter 13 Trace metals in tree rings: What do they tell us?, *in* Markert, B., and Friese, K., eds., Trace Metals in the Environment, Volume Volume 4, Elsevier, p. 375-385.

Hutchins-Cabibi, T., Miller, B., Hern, T., and Schwartz, A., 2006, Urban water on the Wasatch Front: Past, present, and future: Western Resources Advocates.

James, L. P., Crittenden, J., M.D., Calkins, F. C., Sharp, B. J., Baker, A. A., and Bromfield, C. S., 1978, Geology of Big Cottonwood Mining District: Utah Geological Survey, State of Utah Department of Natural Resources, scale 1:24000.

Jenny, H., 1994, Factors of soil formation: A system of quantitative pedology, New York, Dover Publications, Inc. .

Kagawa, A., Aoki, T., Okada, N., and Katayama, Y., 2002, Tree-ring Strontium-90 and cesium-137 as potential indicators of radioactive pollution: Journal of Environmental Quality, v. 31, no. 6, p. 2001-2007.

Katayama, Y., Aoki, T., Nagai, M., Nagatomo, T., and Okada, N., 2006, Distribution of 90Sr in the tree rings of a Japanese cedar exposed to the black rain from the Nagasaki atomic bomb: Journal of Radioanalytical and Nuclear Chemistry, v. 267, no. 2, p. 279-286.

Legge, A. H., Kaufmann, H. C., and Winchester, J. W., 1984, Tree-ring analysis by pixe for a historical record of soil chemistry response to acidic air pollution: Nuclear Instruments and Methods in Physics Research Section B: Beam Interactions with Materials and Atoms, v. 3, no. 1–3, p. 507-510.

Li, J., Okin, G., Alvarez, L., and Epstein, H., 2007, Quantitative effects of vegetation cover on wind erosion and soil nutrient loss in a desert grassland of southern New Mexico, USA: Biogeochemistry, v. 85, no. 3, p. 317-332.

Lukaszewski, Z., 1988, The effect of industrial pollution on Zinc, Cadmium and Copper concentration in the xylem rings of Scot's pine (Pinus sylvestris L.) and in the soil: Trees, v. 2, no. 1, p. 1-6.

Naiman, Z., Quade, J., and Patchett, P. J., 2000, Isotopic evidence for eolian recycling of pedogenic carbonate and variations in carbonate dust sources throughout the southwest United States: Geochimica et Cosmochimica Acta, v. 64, no. 18, p. 3099-3109.

NASA/GSFC/Earth Science Data and Information System, E., Land Atmosphere Near-real time Capability for EOS (LANCE) system.

Neff, J. C., Ballantyne, A. P., Farmer, G. L., Mahowald, N. M., Conroy, J. L., Landry, C. C., Overpeck, J. T., Painter, T. H., Lawrence, C. R., and Reynolds, R. L., 2008, Increasing eolian dust deposition in the western United States linked to human activity: Nature Geoscience, v. 1, no. 3, p. 189-195.

Padilla, K. L., and Anderson, K. A., 2002, Trace element concentration in tree-rings biomonitoring centuries of environmental change: Chemosphere, v. 49, no. 6, p. 575-585.

Painter, T. H., Barrett, A. P., Landry, C. C., Neff, J. C., Cassidy, M. P., Lawrence, C. R., McBride, K. E., and Farmer, G. L., 2007, Impact of disturbed desert soils on duration of mountain snow cover: Geophys. Res. Lett., v. 34, no. 12, p. L12502.

Parker, F. W., and Truog, E., 1920, The relation between the calcium and the nitrogen content of plants and the function of calcium: Soil Science, v. 10, no. 1, p. 49-56.

Rabenhorst, M. C., 1984, Airborne dusts in the Edwards Plateau Region of Texas: Soil Science Society of America Journal, v. 48, no. 3, p. 521-627.

Reynolds, A. C., Quade, J., and Betancourt, J. L., 2012, Strontium isotopes and nutrient sourcing in a semi-arid woodland: Geoderma, v. 189–190, no. 0, p. 574-584.

Reynolds, R., Belnap, J., Reheis, M., Lamothe, P., and Luiszer, F., 2001, Aeolian dust in Colorado Plateau soils: Nutrient inputs and recent change in source: Proceedings of the National Academy of Sciences of the United States of America, v. 98, no. 13, p. 7123-7127.

Reynolds, R., Mordecai, J., Rosenbaum, J., Ketterer, M., Walsh, M., and Moser, K., 2010, Compositional changes in sediments of subalpine lakes, Uinta Mountains (Utah): Evidence for the effects of human activity on atmospheric dust inputs: Journal of Paleolimnology, v. 44, no. 1, p. 161-175.

Reynolds, R., Neff, J., Reheis, M., and Lamothe, P., 2006, Atmospheric dust in modern soil on aeolian sandstone, Colorado Plateau (USA): Variation with landscape position and contribution to potential plant nutrients: Geoderma, v. 130, no. 1–2, p. 108-123.

Rhoades, C., Elder, K., and Greene, E., 2010, The influence of an extensive dust event on snow chemistry in the southern Rocky Mountains: Arctic, Antarctic, and Alpine Research, v. 42, no. 4, p. 497-497.

Sheppard, J. C., and Funk, W. H., 1975, Trees as environmental sensors monitoring long-term heavy metal contamination of Spokane River, Idaho: Environmental Science & Technology, v. 9, no. 7, p. 638-642.

Silkin, P. P., and Ekimova, N. V., 2012, Relationship of strontium and calcium concentrations with the parameters of cell structure in Siberian spruce and fir tree-rings: Dendrochronologia, v. 30, no. 2, p. 189-194.

Speer, J., 2010, Fundamentals of tree-ring research, Tuscon, The University of Arizona Press.

Steenburgh, J. W., Massey, J. D., and Painter, T. H., 2012, Episodic dust events of Utah's Wasatch Front and adjoining region: Journal of Applied Meteorology and Climatology, v. 51, p. 1654-1669.

Stewart, B. W., Capo, R. C., and Chadwick, O. A., 1998, Quantitative strontium isotope models for weathering, pedogenesis and biogeochemical cycling: Geoderma, v. 82, no. 1-3, p. 173-195.

UDAQ, U. D. o. A. Q., 2011, 2011 Annual Report, p. 41.

Van der Hoven, S. J., and Quade, J., 2002, Tracing spatial and temporal variations in the sources of calcium in pedogenic carbonates in a semiarid environment: Geoderma, v. 108, no. 3-4, p. 259-276.

Vogel, T. A., Cambray, F. W., and Constenius, K. N., 2001, Origin and emplacement of igneous rocks in the central Wasatch Mountains, Utah: Rocky Mountain Geology, v. 36, no. 2, p. 119-162.

Warren, S. G., and Wiscombe, W. J., 1980, A model for the spectral albedo of snow. II: snow containing atmospheric aerosols: Journal of the Atmospheric Sciences, v. 37, no. 12, p. 2734 - 2745.

Watmough, S. A., 1999, Monitoring historical changes in soil and atmospheric trace metal levels by dendrochemical analysis: Environmental Pollution, v. 106, no. 3, p. 391-403.

Watmough, S. A., and Hutchinson, T. C., 1996, Analysis of tree rings using inductively coupled plasma mass spectrometry to record fluctuations in a metal pollution episode: Environmental Pollution, v. 93, no. 1, p. 93-102.

West, L. T., 1988, Calciustolls in central Texas: II. Genesis of calcic and petrocalcic horizons: Soil Science Society of America Journal, v. 52, no. 6, p. 1731-1740.

Westerling, A. L., Hidalgo, H. G., Cayan, D. R., and Swetnam, T. W., 2006, Warming and earlier spring increase western U.S. forest wildfire activity: Science, v. 313, no. 5789, p. 940-943.

Zayed, J., 1992, Variations of trace element concentrations in red spruce tree rings: Water, Air and Soil Pollution, v. 65, no. 3-4, p. 281-291.

Zobitz, J. M., Keener, J. P., Schnyder, H., and Bowling, D. R., 2006, Sensitivity analysis and quantification of uncertainty for isotopic mixing relationships in carbon cycle research: Agricultural and Forest Meteorology, v. 136, no. 1–2, p. 56-75.